

**PREPARATION AND PHYSICAL
CHARACTERIZATION OF CLAY/EPDM
NANOCOMPOSITES**

A Thesis Submitted to
the Graduate School of Engineering and Sciences of
İzmir Institute of Technology
in Partial Fulfillment of the Requirements for the Degree of

MASTER OF SCIENCE

in Material Science and Engineering

by
Çiçek KARŞAL

July 2008
İZMİR

ACKNOWLEDGEMENT

I would like to express my gratitude to my advisor Assoc. Prof. Dr. Metin Tanođlu and my co-advisor Assoc. Prof. Dr. Lutfi Özyüzer for their invaluable advice, guidance, and encouragement. I also thank to Assoc. Prof. Dr. Funda Tihminliođlu for her support.

I would like to thank the Center for Materials Research staff at Izmir Institute of Technology for their help and patience during my study.

I would like to acknowledge The Scientific and Technical Research Council of Turkiye (TUBİTAK) for financial support to 106M157 project for their support to my study.

A special thank go to Sibel Odabaş, Nursel Karakaya and Osman G. Ersoy from Arçelik A.Ş. Research and Development Center for providing the materials and the mechanical test machines, also for their advice throughout my study.

I am especially grateful to my laboratory colleagues for their encouragement, help and patience.

I offer sincere thanks to my family for their support and continuous advice throughout my education and their unlimited patience. I am also grateful for their invaluable love and understanding for all my life.

ABSTRACT

PREPARATION AND PHYSICAL CHARACTERIZATION OF CLAY/EPDM NANOCOMPOSITES

Polymer/clay nanocomposites have been extensively studied in recent years because they often exhibit improved properties different from their micro and macrocomposite counterparts. Addition of organophilic layered silicates to the polymer produces effective polymer nanocomposites by intercalation of macromolecules into the interlayer spaces. The performance of polymer/clay composites is not only related to the nature of the clay but also to the reinforcing mechanism of filler and the preparation conditions.

In this study, the effects of mixing conditions and effect of aging on mechanical, physical and thermal properties of ethylene-propylene-diene rubber (EPDM)/Organo modified montmorillonite (OMMT) nanocomposites were studied at two different clay loadings 5 wt.% and 10 wt.%. EPDM/OMMT nanocomposites were prepared by melt blending method. The experimental results of X-ray diffraction (XRD) and scanning electron microscopy showed that the organically modified MMT existed in the form of an intercalated structure and that was exfoliated in EPDM matrix depending on the mixing conditions. XRD patterns showed that the interlayer distance of the organically modified clay was 30.9Å, which was larger than those of the unmodified clay (14.6Å). The mechanical evaluation of the nanocomposites was performed by tensile and tear testing. The mechanical tests showed that the properties of nanocomposites were significantly improved with addition of OMMT. The effects of the processing conditions were manifested in both the morphology and mechanical properties, which showed significant increase when optimized process conditions are applied. In addition, chemical test was performed on the nanocomposites to monitor the degradation of the mechanical properties. It was found that the reduction of the mechanical properties of nanocomposites after aging process is lower as compared to those of neat EPDM.

ÖZET

KİL/EPDM NANOKOMPOZİTLERİNİN HAZIRLANMASI VE FİZİKSEL KARAKTERİZASYONU

Kil/polimer nanokompozitler, mikro ve makro yapıları kompozitlerden farklı olarak daha gelişmiş özellikler sergilemelerinden son yıllarda yaygın olarak çalışılmaktadır. Organofilik özellik kazandırılmış tabakalı silikatların polimer matriksine eklenmesi, makromoleküllerin tabakalar arasında dağılımıyla etkin polimer nanokompozitler elde edilmesini sağlar. Kil/polimer kompozitlerinin performansı, sadece kilin doğasına değil, aynı zamanda dolgu bileşenlerinin güçlendirme mekanizması ve üretim koşullarıyla da ilgilidir.

Üretim koşullarının ve yaşlandırmanın etilen-propilen- dien kauçuğu (EPDM)/organo modifiye edilmiş montmorilonit (OMMT) nanokompozitlerinin fiziksel, mekanik ve termal özellikleri üzerindeki etkisi, ağırlıkça % 5 ve 10 kil ilavesiyle incelenmiştir. Kil/EPDM nanokompozitleri eriyik ile dağılım yöntemiyle üretilmiştir. X-ışını kırınımı ve taramalı elektron mikroskobu ile yapılan gözlemler sonucunda, modifikasyona tabi tutulmuş montmorilonit kilinin (OMMT) dağılım tabakalı yapı halinde, üretim koşullarına bağlı olarak EPDM matriksi içinde ise tamamen dağılmış olduğu görülmüştür. XRD, hiçbir muameleye tabi tutulmamış kilin tabakalar arası mesafesinin 14.6 Å iken modifikasyon işlemi ile bu mesafenin 30.9 Å'a çıktığını göstermektedir. Kauçuk nanokompozitlerinin mekanik gelişimleri, çekme ve yırtılma testleri ile incelenmiştir. Mekanik testler, modifiye edilmiş kil ilavesinin nanokompozitlerin özelliklerini önemli ölçüde artırdığını göstermektedir. Morfolojik ve mekanik özellikler üzerinde proses koşullarının doğru kombinasyonu ile elde edilen önemli artış, proses koşullarının açıkça etkili olduğunu gösterir. Bunların yanında, mekanik özelliklerdeki değişimi incelemek amacıyla yaşlandırma testi gerçekleştirilmiştir. Buna göre, yaşlandırma sonrasında nanokompozitlerin mekanik özellikleri, saf EPDM'e göre daha yüksek sonuç vermiştir.

TABLE OF CONTENTS

LIST OF FIGURES	viii
LIST OF TABLES	xii
CHAPTER 1. INTRODUCTION	1
CHAPTER 2. NANOCOMPOSITES	4
2.1. Nanocomposite Preparation Methods	5
2.2. Types of Nanocomposite Structure	6
2.3. Structure and Properties of Layered Silicates	7
2.3.1. Inorganic Montmorillonite	9
2.3.2. Organically Modification Montmorillonite	11
2.4. Elastomeric Materials	12
2.4.1. Ethylene Propylene Diene Rubber (EPDM)	13
2.4.1.1. Ethylene-Propylene Composition	14
2. 4.1.2. Diene Content	15
2. 4.1.3. Crosslinking (Vulcanization) Systems	16
2. 4.1.3.1. Sulfur Vulcanization	18
2. 4.1.3.2. Peroxide Vulcanization	19
2.5. Properties of EPDM/Layered Clay Nanocomposites	20
2.5.1. Microstructural Properties of EPDM/Layered Clay Nanocomposites	20
2.5.2. Mechanical Properties of EPDM/Layered Clay Nanocomposites	23
2.5.3. Thermal Properties of EPDM/Layered Clay Nanocomposites	25
CHAPTER 3. EXPERIMENTAL	28
3.1. Materials	28
3.2. Modification of Clay	29
3.3. Preparation of EPDM/Clay Nanocomposites	30
3.4. Characterization of Nanocomposites	32
3.4.1. Morphological Investigation	32

3.4.1.1. X-ray Diffraction (XRD).....	32
3.4.1.2. Scanning Electron Microscopy (SEM).....	32
3.4.1.3. Fourier Transform Infrared Spectroscopy (FTIR).....	32
3.4.2. Measurement of Mechanical Properties.....	33
3.4.2.1. Tensile Test	33
3.4.2.2. Tear Test.....	33
3.4.2.3. Hardness Measurements.....	34
3.4.2.4. Aging Test	34
3.4.3. Measurement of Thermal Properties	34
3.4.3.1. Differential Scanning Calorimetry (DSC)	35
3.4.3.2. Thermogravimetric Analysis (TGA)	35
3.4.3.3. Dynamic Mechanical Analysis.....	35
CHAPTER 4. RESULTS AND DISCUSSION.....	36
4.1. Investigation of Intercalation and Dispersion of Clay Layers	36
4.1.1. Examination of the Morphology of the Nanocomposites	42
4.1.2. Fourier Transform Infrared Spectroscopy.....	46
4.2. Mechanical Properties of EPDM/Layered Clay Nanocomposites.....	48
4.2.1. Tensile Properties of EPDM/Layered Clay Nanocomposites and Effects of Aging Conditions.....	48
4.2.1.1. Effect of Blending Time on the Mechanical Properties	48
4.2.1.2. Effect of Blending Temperature on the Mechanical Properties	53
4.2.1.3. Effect of Blending Speed on the Mechanical Properties.....	55
4.2.2. Hardness of Nanocomposites and Influence of Aging Test on Hardness	58
4.2.3. Tear Properties of EPDM/Layered Clay Nanocomposites	60
4.3. Thermal Properties of Nanocomposites	62
4.3.1. Thermogravimetric Analysis (TGA).....	62
4.3.2. Differential Scanning Calorimeter (DSC).....	64
4.3.3. Dynamical Mechanical Analysis (DMA).....	66
CHAPTER 5. CONCLUSION	68
REFERENCES	71

LIST OF FIGURES

<u>Figure</u>	<u>Page</u>
Figure 2. 1. Schematic of the polymer layered silicate nanocomposite morphologies: (a) miscible or unmixed conventional composite system, (b) intercalated systems and (c) exfoliated or delaminates system.....	7
Figure 2. 2. Structure of 1:1 phyllosilicates.....	8
Figure 2. 3. Structure of 2:1 phyllosilicates.....	8
Figure 2. 4. Structure of montmorillonite.....	10
Figure 2. 5. Schematic illustration of surface modification of montmorillonite.....	12
Figure 2. 6. Structure of (a)ethylene, (b)propylene and (c)copolymer of ethylene and propylene.....	13
Figure 2. 7. Commercially used diene containing monomers: (a) 1,4 hexadiene, (b) ethylidene norbornene (ENB) and (c) dicyclopentadiene (DCDP).....	15
Figure 2. 8. Crosslinking process.....	17
Figure 2. 9. Structural features of a sulfur vulcanized rubber.....	18
Figure 2.10. XRD patterns of: (a) organoclay (2 g), (b) EPDM (100 phr) + organoclay (3 phr) and (c) MAH-g EPDM (100 phr) + organoclay (3 phr).....	21
Figure 2.11. Transmission electron micrographs of (a) EPDM (100 phr) + organoclay (3 phr) and (b) MAH-g EPDM (100 phr) + organoclay (3 phr).....	22
Figure 2.12. XRD patterns of a) octadecylammonium modified MMT and b-f) EPDM/clay nanocomposites used five types of vulcanization accelerators: b) thiourea (NPV/C), c) 2-mercaptobenzothiazole(MBT), d) N-cyclohexyl-2-sulfonamide(CZ), e)tetra- methylthiuram monosulfide (TS) and f) zinc dimethyldithiocarbamate (PZ).....	23

Figure 2.13. Isothermal DSC thermograms for EPDM composites with various organoclay loading.....	26
Figure 2.14. TGA thermograms of unfilled EPDM and 10% filled EPDM nanocomposite	27
Figure 3. 1. Structure of (a) EPDM containing ENB, (b) octadecylamine	29
Figure 3. 2. Schematic illustration of surface modification of montmorillonite	30
Figure 3. 3. Haake Mixer	31
Figure 3. 4. Two roll mill.....	31
Figure 3. 5. Schematic illustration of production of EPDM/clay nanocomposites	31
Figure 3. 6. Photo of tensile test and tensile test specimen.....	33
Figure 3. 7. Tear test specimen before and after the tear test	33
Figure 3. 8. The equipment used for aging experiment	34
Figure 3. 9. DSC equipment.....	35
Figure 3.10. DMA equipment.....	35
Figure 4. 1. XRD patterns of Na ⁺ -montmorillonite and organo modified montmorillonite	37
Figure 4. 2. XRD pattern of neat EPDM between a) $2\theta=5-70^\circ$, b) $2\theta=1-12^\circ$	38
Figure 4. 3. XRD patterns of EPDM/ 5 wt. % OMMT nanocomposites with 10, 15 and 20 min blending time(blending temperature= 150°C , blending speed= 90 rpm).....	39
Figure 4. 4. XRD patterns of EPDM/ 10 wt. % OMMT nanocomposites with 10, 15 and	39
Figure 4. 5. XRD patterns of EPDM/ 5 wt. % OMMT nanocomposites with 120 and 150°C blending temperature (blending time= 15 min , blending speed= 90 rpm).....	40
Figure 4. 6. XRD patterns of EPDM/ 10 wt. % OMMT nanocomposites with 120 and 150°C blending temperature (blending time= 15 min , blending speed= 90 rpm).....	40
Figure 4.7. XRD patterns of EPDM/ 5 wt. % OMMT nanocomposites with 60 and 90 rpm blending speed (blending time= 15 min , blending temperature= 150°C)	41

Figure 4. 8. XRD patterns of EPDM/ 10 wt. % OMMT nanocomposites with 60 and 90 rpm blending speed (blending time=15 min, blending temperature=150°C)	42
Figure 4. 9. Backscattered SEM fracture surface micrograph of neat EPDM after tensile testing.....	43
Figure 4.10. Backscattered SEM fracture surface micrographs of EPDM/ 5 wt. % OMMT nanocomposite blended for a) 10, b) 15 and c) 20 min.....	43
Figure 4. 11. Backscattered SEM fracture surface micrographs of EPDM/ 5 wt. % OMMT nanocomposite blended at a) 120 and b) 150°C	44
Figure 4. 12. Backscattered SEM fracture surface micrographs of EPDM/ 5 wt. % OMMT nanocomposite blended with a)60 and b) 90 rpm.....	44
Figure 4. 13. Backscattered SEM fracture surface micrographs of EPDM/ 10 wt. % OMMT nanocomposite blended for a) 10, b) 15 and c) 20 min.....	45
Figure 4. 14. Backscattered SEM fracture surface micrographs of EPDM/ 10 wt. % OMMT nanocomposite blended at a) 120 and b) 150°C	46
Figure 4. 15. Backscattered SEM fracture surface micrographs of EPDM/ 10 wt. % OMMT nanocomposite blended with a)60 and b) 90 rpm.....	46
Figure 4. 16. SEM image and the corresponding maps of carbon, oxygen, silicon, aluminum, sodium, sulfur and zinc elements from the same surface	47
Figure 4. 17. FTIR spectra for (a)pure MMT, (b)surfactant (octadecylamine) and (c) organically modified MMT (OMMT).....	48
Figure 4. 18. Prior to aging, tensile strength values of neat EPDM and its nanocomposites containing 5 and 10 wt. % of OMMT with respect to various blending times including 10, 15 and 20 min.	50
Figure 4. 19. After aging process tensile strength values of neat EPDM and its nanocomposites containing 5 and 10 wt. % of OMMT with respect to various blending times including 10, 15 and 20 min.	50
Figure 4. 20. Prior to aging, tensile strength values of neat EPDM and its nanocomposites containing 5 and 10 wt. % of OMMT with respect to blending temperatures of 120 and 150°C	53

Figure 4. 21. After aging, tensile strength values of neat EPDM and its nanocomposites containing 5 and 10 wt. % of OMMT with respect to blending temperatures of 120 and 150°C	54
Figure 4. 22. Prior to aging, tensile strength values of neat EPDM and its nanocomposites containing 5 and 10 wt. % of OMMT with respect to blending speeds of 60 and 90 rpm.....	57
Figure 4. 23. After aging, tensile strength values of neat EPDM and its nanocomposites containing 5 and 10 wt. % of OMMT with respect to blending speeds of 60 and 90 rpm.....	57
Figure 4. 24. Effect of clay addition and aging on hardness values of EPDM and its nanocomposites.....	58
Figure 4. 25. Tear strength values for neat EPDM and its nanocomposites containing 5 and 10 wt. % OMMT blended for 10, 15 and 20 min.....	60
Figure 4. 26. Tear strength values for neat EPDM and its nanocomposites containing 5 and 10 wt. % OMMT and blended of 120 and 150 min.....	61
Figure 4. 27. Tear strength values for neat EPDM and its nanocomposites containing 5 and 10 wt. % OMMT blended with rotor speed of 60 and 90 rpm.....	61
Figure 4. 28. The effect of organoclay (OMMT) content on the TGA thermograms of EPDM.....	63
Figure 4. 29. Typical TGA thermogram and its derivative curves of neat EPDM and EPDM/OMMT nanocomposites.....	63
Figure 4. 30. DSC thermograms for neat EPDM and its nanocomposites containing 5 and 10 wt. % OMMT.....	65
Figure 4. 31. Dynamic mechanical analysis (DMA) spectra: a) Storage modulus (E') and b) $\tan \delta$ as a function of temperature for the neat EPDM and its nanocomposites containing 5 and 10 wt. % OMMT.....	67

LIST OF TABLES

<u>Table</u>	<u>Page</u>
Table 2. 1. Classifications of layered silicate crystals	7
Table 2. 2. The additives of natural rubber	18
Table 2. 3. Mechanical properties of EPDM/organoclay (10 phr) compounds, prepared under different conditions with and without MAgEPDM compatibilizer.....	25
Table 3. 1. Details of materials used.....	28
Table 3. 2. Composition of neat EPDM and EPDM/OMMT nanocomposites.....	32
Table 4. 1. Loss in tensile strength after aging test.....	51
Table 4. 2. Effect of aging, mixing time and the OMMT content on elongation at break, modulus at 100% extension and tear strength for neat EPDM and EPDM/OMMT nanocomposites (Standart deviations are given in parenthesis)	52
Table 4. 3. Loss in tensile strength after aging test.....	54
Table 4. 4. Effect of temperature on elongation at break and modulus at 100% extension for neat EPDM and EPDM/OMMT nanocomposites (Standart deviations are given in parenthesis)	56
Table 4. 5. Loss in tensile strength after aging test.....	58
Table 4. 6. Effect of aging, rotor speed and the OMMT content on elongation at break and modulus at 100% extension for neat EPDM and EPDM/OMMT nanocomposites (Standart deviations are given in parenthesis)	59
Table 4. 7. Decomposition temperatures of neat EPDM and OMMT nanocomposites prepared with various content and processing conditions.....	64
Table 4. 8. Glass transition temperatures (T_g) of EPDM and its nanocomposites processed under various conditions	65

CHAPTER 1

INTRODUCTION

The materials which can meet difficult conditions with better performance to cost ratio have been demanded by large number of industrial applications. Polymer-layered clay nanocomposites have recently attracted significant research interest due to their improved strength and modulus, better thermal and chemical stabilities and enhancement of flame retardancy (Liu, et al. 2006, Giannelis 1998, Ahmadi and Huang 2005). The improved properties can be obtained if a relatively better dispersion of clay layers in the polymer matrix can be achieved. A strong interfacial interaction between the clay surfaces and polymer matrix is expected to occur (Liu, et al. 2006 and Kurian, et al. 2004). A great number of polymer-clay composite systems have been studied based on such as epoxy resins (Bozkurt, et al. 2007, Wang and Pinnavaia 1994, Van and Pinnavaia 1994, Kelly, et al. 1994), polyimide (Yano, et al. 1993), polystyrene (Vaia, et al. 1993, Vaia, et al. 1995, Moet and Akelah 1993, Weiner, et al. 1999, Hasegawa, et al. 1999), polyurethane (Zilg, et al. 1999), poly(ethylene terephthalate) (Ke, et al. 1999) and polyolefins (Usuki, et al. 1997, Kawasumi, et al. 1997, Hasegawa, et al. 1998).

Ethylene propylene diene terpolymer (EPDM) is a member of unsaturated polyolefins which is one of the most widely used polymers in industry (Ahmadi, et al. 2005, Usuki, et al. 2002). It has been extensively applied in applications such as automotive weather-stripping and seals, radiator hoses, electrical insulation, roofing membrane, tubing, belts, house-hold applications and other general-purpose applications and sporting goods (Ahmadi, et al. 2005, Acharya, et al. 2004). However, it is difficult to disperse the clay layers within EPDM, because EPDM does not have any polar group in its backbone and it is incompatible with polar organophilic clay to prepare products having desired properties (Liu, et al. 2006, Ahmadi, et al. 2005, Ma, et al. 2006, Zheng, et al. 2004).

Clay is comprised of layered silicates that have about 1 nm layer thickness with a high surface area and high ion exchange capacity. Because of the layered structure bonded with weak bonding forces, silicate layers may be dispersed in a polymer matrix at the nanometric level (Lipoittevin, et al. 2003, Lew, et al. 2004). The clay minerals

have Na^+ , Ca^{2+} or Mg^{2+} cations which are hydrated in the interlayer spacing. One of the most commonly used organically layered silicates is derived from montmorillonite (MMT).

Homogeneous dispersion the organophobic layered clay mineral in an organic polymer matrix, especially in the absence of high shearing forces, may only be achievable through strategies that promote favorable interactions between the matrix and the clay surfaces. This includes the use of some compatibilizing surfactants. An ion-exchange reaction occurs with the cationic surfactants including primary, secondary, tertiary and quaternary alkyl ammonium cations. Alkyl ammonium cations lower the surface energy of inorganic component and improve the wetting characteristics of the polymer matrix, and result in a larger interlayer spacing (Mohammad and Simon 2006). A number of surfactants containing ammonium cations have been studied to modify the clay surfaces. Their influence on the morphology and mechanical properties of the EPDM/OMMT nanocomposites has been reported (Gatos, et al. 2004). Gatos and Karger-Kocsis (Gatos and Karger-Kocsis, et al. 2005) have been devoted that increasing the polarity of the EPDM has favored the intercalation/exfoliation of the organoclay irrespective to the type of its intercalant (primary or quaternary). They have also investigated the EPDM nanocomposites processed with the EPDMgMA. They have found that the clay dispersion in EPDM composites with EPDMgMA (maleic anhydride grafted ethylene propylene diene terpolymer) is finer and has higher strain values as compared to the EPDM nanocomposites processed without the EPDMgMA (Gatos and Karger-Kocsis, et al. 2005). Usuki, et al. (Usuki, et al. 1997) have reported that thiuram (tetramethylthiuram monosulfide) and dithiocarbamate (zinc dimethyldithiocarbamate) used as the vulcanization accelerator showed superior properties. However, when thiourea (ethylenethiourea), thiazole (2-mercaptobenzothiazole), and sulfonamide (N-cyclohexyl-2 benzothiazylsulfenamide) were used as accelerators, the dispersibility of clays in EPDM was found to be insufficient. EPDM nanocomposites prepared by two different melt blending methods (direct and indirect) were compared by Ahmadi et al. (Ahmadi, et al. 2005). In the indirect method, the EPDMgMA was first melt-mixed with organoclay to yield organoclay intercalated EPDMgMA. Then, EPDM and the prepared blend were melt-mixed to obtain EPDM/OMMT nanocomposites. In the direct method, all of the materials (EPDM, EPDMgMA, and OMMT) were melt-blended in one stage. As a result, the direct method was found to be more sufficient because of its low cost, feasibility and simplicity because it was found that the properties of nanocomposites by

these two methods were nearly same. However, there is no work reported in the literature on the effects of processing conditions and aging environment on the properties of EPDM/clay nanocomposites with EPDMgMA.

In this study, EPDM and its nanocomposites containing 5 wt.% and 10 wt.% organomodified montmorillonite were produced by melt intercalation method at different processing conditions. The effects of the process parameters and the chemical (detergent) aging on the mechanical, physical and thermal properties of organoclay reinforced EPDM were investigated. The effects of modification of the clay particles on the nanocomposite morphology were investigated by scanning electron microscopy and X-ray diffraction techniques. Tensile and tear tests were performed to investigate the aging effect on nanocomposites.

CHAPTER 2

NANOCOMPOSITES

The materials with better performances in many different areas of applications have been demanded by large number of industries. Nanocomposites are the materials that are manufactured by the dispersion of nanoparticles into the macroscopic materials. Nanocomposites have recently attracted significant research interest due to their improved strength and modulus, better thermal and chemical stabilities with enhanced flame retardancies (Liu, et al. 2006, Giannelis, et al. 1998). Having such improved properties make nanocomposites attractive in various applications such as automotive, food, construction, household, medical, agricultural and space industries in the production of films, engine covers, oxygen, gas barriers and etc.

The scientific and industrial interests have been devoting to polymer nanocomposites in recent years. They often exhibit remarkable improvement in materials properties when compared to virgin polymer or conventional composites. Various nano reinforcements currently being developed are nanoclay, cellulose nanowhiskers, ultra fine layered titanate and carbon nanotubes.

Clay minerals as a reinforcing material in polymer matrix have been widely used because of their low cost and availability (Acharya, et al. 2004). These systems appear as a new class of materials in which inorganic particles with nanoscale dimension are dispersed in the organic polymer matrix. Because of their nanoscale size and interfacial interaction between the matrix and layered clay, these nanocomposites exhibit higher mechanical properties, enhanced thermal stability and improved chemical stability than those of conventional micro composite counterparts (Zheng, et al. 2004).

The improved properties can be obtained when better dispersion of clay layers in the polymer matrix can be achieved. A strong interfacial interaction between the clay surfaces and polymer matrix occurs as a result of dispersion (Liu, et al. 2006). A great number of polymer-clay composite systems have been studied based on such as epoxy resins (Bozkurt, et al. 2007, Kelly, et al. 1994), polyimide (Yano, et al. 1993), polystyrene (Vaia, et al. 1993, Hasegawa, et al. 1999), polyurethane (Zilg, et al. 1999), poly(ethylene terephthalate) (Ke, et al. 1999) and polyolefins (Usuki, et al. 1997, Hasegawa, et al. 2000). Although clay nanocomposites have been prepared and tested

for many thermoplastics and thermosetting polymers, much less attention has been given to rubber/clay nanocomposites.

Rubbers with their low modulus stand to gain much in terms of modulus and strength from the addition of nanoparticles. In addition, the effect of clay addition on rubber tensile and tear properties is under research. The further results show significant improvements in mechanical and thermal properties that will be beneficial in many different industries such as construction, automotive and household applications.

2.1. Nanocomposite Preparation Methods

One successful method to prepare polymer/layered silicate nanocomposites is to intercalate polymers into silicate galleries. In general, intercalation of polymer chains into the silicate galleries is done by using one of the following processing techniques:

In-situ polymerization Method: In this method, layered silicate is swollen within the liquid monomer solution so the formation of polymer can occur between and around the intercalated layers. The polymerization can be initiated either by the incorporation of curing agent, initiator or by increasing the temperature if it is sufficiently reactive.

Solution Blending Method: This method is based on a solvent system in which the polymer is soluble and the silicate layers are swellable. The layered silicate is first swollen in a solvent. When the polymer and layered silicate solutions are mixed, the polymer chains intercalate and displace the solvent within the interlayer of the silicate. Upon solvent removal, the intercalated structure remains, resulting in nanocomposite. Using this method, intercalation only occurs for certain polymer/solvent pairs. The disadvantages of this method are the use of environmentally unfriendly and economically prohibitive organic solvents.

Melt Intercalation Method: The melt intercalation technique has become the standard for polymer/layered silicate nanocomposites and is also quite compatible with the industrial techniques. In this method polymer and modified layered silicate mixture are blended in the molten state under shear. The polymer chains reptate form the molten mass into the silicate galleries to form either intercalated or delaminated nanocomposites.

Latex Compounding Method: This method is also a promising method in mostly rubber/layered silicate nanocomposites. Latex compounding technique starts with dispersing layered silicates in water acts as a swelling agent owing to hydration of the intergallery cations. Rubber latex is then added and mixed for a period of time, with the dispersion of layered silicate in water followed by coagulation.

2.2. Types of Nanocomposite Structure

The incorporation of a few weight percent of modified layered silicates which are properly dispersed in the polymer matrix can result in very high surface areas for polymer/layered silicate interactions, as compared to the conventional polymer/filler composites. According to the strength of the interfacial between polymer matrix and layered silicate four type of polymer/clay composites can be produced (Mohammad and Simon 2006).

Conventional composites: In a conventional polymer composite, as represented in Figure 2.1.a layered silicate acts as a conventional, micron sized fillers such as carbon black clusters or other inorganic fillers.

Intercalated nanocomposite: Intercalated nanocomposites are formed by the insertion of a rubber chains between the unaltered silicate layers, maintaining their regular alternation of galleries and laminas (Figure 2.1.b).

Exfoliated nanocomposite: In exfoliated nanocomposites the individual layers of the nanoclay are totally delaminated and dispersed in the rubber matrix as shown in Figure 2.1.c. The ordered structure of layered silicate is lost and the average distances between the exfoliated layers depend on clay loading.

Intermediate nanocomposites: Rubber-clay nanocomposites which are partially intercalated and partially exfoliated, are an intermediate type of nanocomposite.

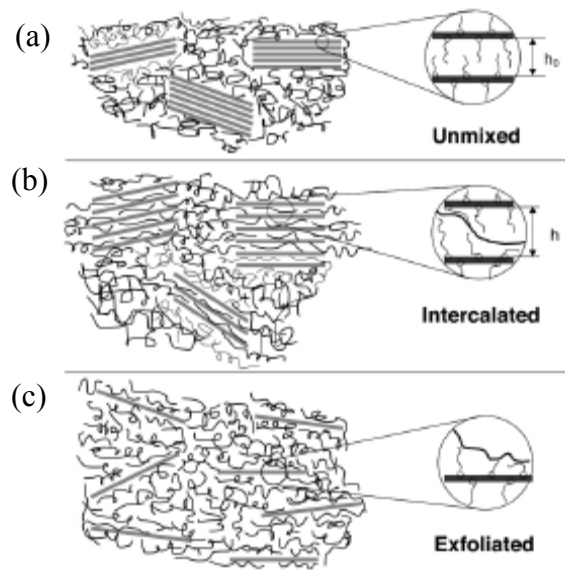


Figure 2.1. Schematic of the polymer layered silicate nanocomposite morphologies: (a) miscible or unmixed conventional composite system, (b) intercalated systems and (c) exfoliated or delaminates system (Source: Mohammad and Simon 2006)

2.3. Structure and Properties of Layered Silicates

The geologic term clay refers to any naturally occurring material with a particle size less than 2 microns. Sheet silicates or clay minerals are the largest group of two-dimensional structures. According to the relative ratio two unit crystal sheets in Table 2.1, the layered silicates are divided into three types.

Table 2.1. Classifications of layered silicate crystals
(Source: Bruce and O’Hare 1996)

Unit crystal lamellae type	Family of clay	Examples of clay
1:1	Family of kaolinite Family of illite	Kaolinite, perlite clay, etc. Illite, etc.
2:1	Family of saponite Family of hydromica	Montmorillonite, saponite, vermiculite Illite, glauconite
2:2	Chlorite family and others	Chlorite
Mixed layer and chain structure	Family of saponite	Sepiolite, palygorskite, attapulgite

1:1 arrangement has alternating tetrahedral and octahedral sheets as seen in Figure 2.1. The main bonding forces between the layers are hydrogen bonds between –OH on one layer and a bridging -O- on the next.

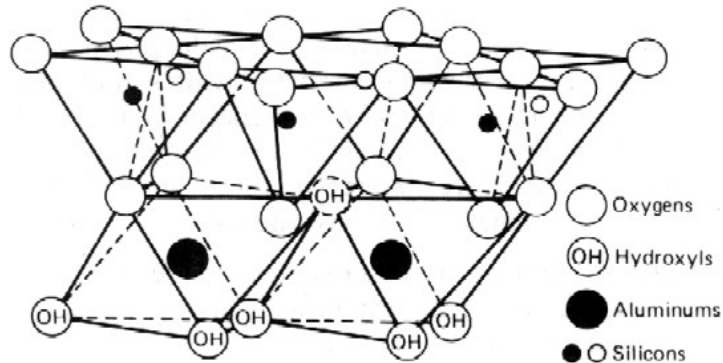


Figure 2.2. Structure of 1:1 phyllosilicates
(Source: Bruce and O’Hare 1996)

2:1 arrangement has repeating units of tetrahedral layers. Its unit is composed of two crystal sheets of silica tetrahedron combined with one crystal sheet of alumina octahedron between them as shown in Figure 2.3.

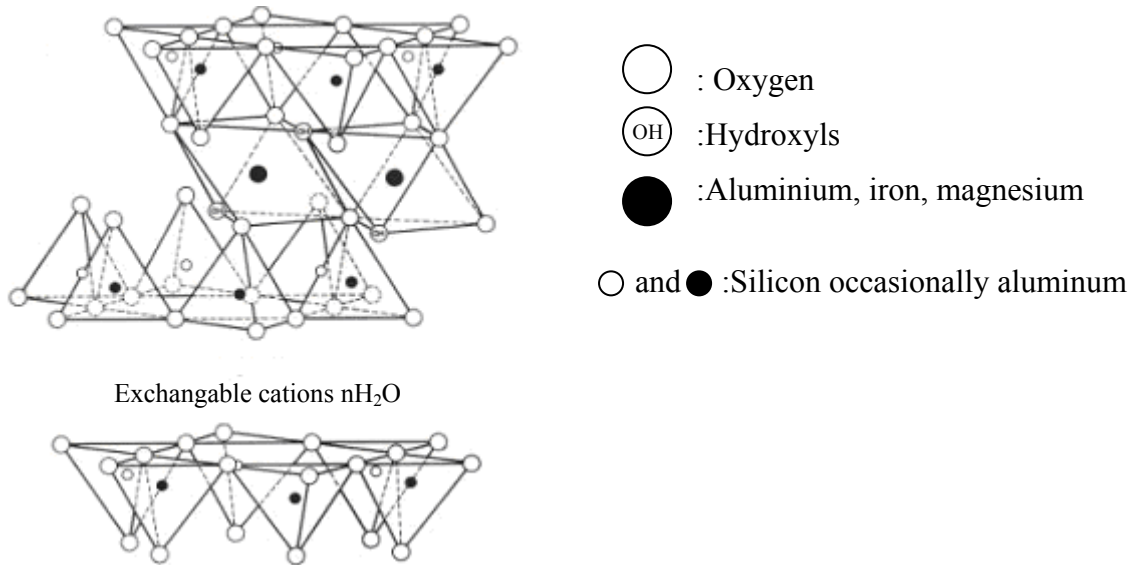


Figure 2.3. Structure of 2:1 phyllosilicates
(Source: Bruce and O’Hare, 1996)

In 2:2 arrangement, its unit lamellar crystal is composed of four crystal sheets, in which crystal sheets of silica tetrahedron and alumina or magnesium octahedron are alternately arranged.

In Mixed lamellar and chain-like structure, the lamellar hexagon rings composed of silica tetrahedron sheets are arranged opposite to one another in a right direction from the top down.

The commonly used layered silicates for the preparation of polymer/layered silicate nanocomposites belong to the same general family of 2:1 phyllosilicates. The layer thickness is around 1 nm and the lateral dimensions of these layers may vary from 30 nm to several microns, depending on the particular layered silicate. Stacking of the layers leads to a regular van der Waals gap between the layers called the interlayer or gallery.

Two particular characteristics of layered silicates that are generally considered for polymer/layered silicate nanocomposites are the ability of the silicate particles to disperse into individual layers, and the ability to ion exchange reactions with organic and inorganic cations (Ma, et al. 2006). Pristine layered silicates usually contain hydrated Na^+ or K^+ ions. To render layered silicates miscible with polymer matrix, the hydrophilic silicate surface must be converted to an organophilic surface.

2.3.1. Inorganic Montmorillonite

Montmorillonite (MMT) is a derivative of pyrophyllite that has the formula of $\text{Al}_4[\text{Si}_4\text{O}_{10}](\text{OH})_2$. It is the most commonly used layered silicates for the preparation of nanocomposites. Its successful candidate to prepare nanocomposites, MMT, is environmentally friendly and naturally abundant. As well as this, it can be broken down into nanoscale (1-nm thick and 100 nm in length) building blocks and uniformly dispersed in the polymer matrix to form exfoliated nanocomposites during the melt blending process. The crystal structure of montmorillonite (MMT) is shown in Figure 2.4.

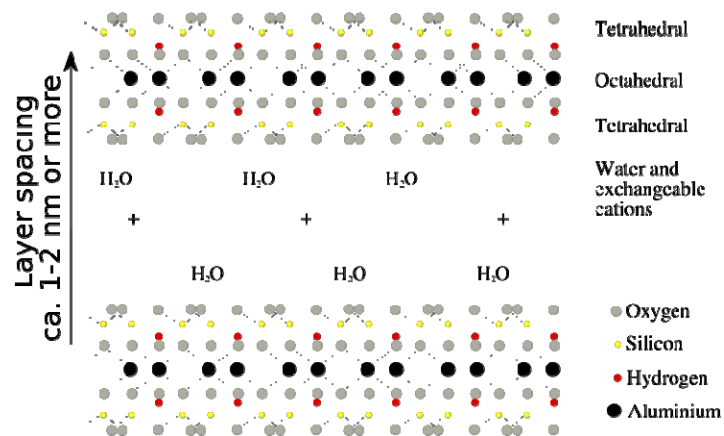


Figure 2.4 Structure of montmorillonite

(Source: Wikipedia 2008)

Montmorillonite is composed of complicated oxides and organic residuals. In these compositions, some cations are usually hydrated inside the layer space of MMTs. These hydrated cations, such as cations of Na^+ , K^+ , Ca^{2+} , Mg^{2+} , Al^{3+} , H^+ , Li^+ , Cs^+ , Rb^+ and NH_4^+ are exchangeable. The type of MMT is usually classified by its exchangeable cations, such as Li-MMTs, in which the MMT contains the exchangeable cations of Li inside its interlayer space, Na-MMTs, which refers to MMTs with Na^+ inside its interlayer space and the Ca-MMTs, which are MMTs with an exchangeable Ca^{2+} inside their layer gallery.

All positions at the top and base of the lattice layers of MMT are completely occupied by oxygen atoms. These layers are held together by a relatively weak intermolecular force. As a result, water molecules easily penetrate the interlayer region and can cause the expansion of the lattice. Owing to isomorphic substitution between metals, MMT with negative charges can adsorb cations with an electric quantity equal to that of montmorillonite. Hydrated cations enter the interlayer region, which then leads to an increase in the distance between adjacent layers. Accordingly, MMT is an expandable clay mineral. The whole surface of layers including the internal surface and external surface can be hydrated and the exchange reaction of cations can occur there. MMT possesses a specific surface area as large as $800 \text{ m}^2 \text{ g}^{-1}$.

The degree of expansion of MMT is determined by the category of the exchangeable cations. The expansion pressure of MMT in which sodium ions constitute the majority of the adsorbed cations (called Na-MMT) is very high, leading to the exfoliation and dispersion of the crystal in the manner of fine particles or even single

layers. The size of the particle has been measured, but this is difficult because the clay mineral is very thin, its shape is irregular and the range of sizes is very wide.

2.3.2. Organically Modification of Montmorillonite

The objectives of modification of layered silicate are flexible dispersion and application to different matrices. The design principles for the modification of selected particles are to improve their compatibility with the matrix and to accelerate the homogeneous distribution. In order to facilitate, the penetration of the chains in between the galleries and thus to form a nanocomposite, different strategies were followed. They include the modification of the surface of the clay layers and/or the polymeric chains. (Ke and Stroeve 2005)

Homogeneous dispersion the organophobic layered clay mineral in an organic polymer matrix, especially in the absence of high shearing forces, may only be achievable through strategies that promote favorable interactions between the matrix and the clay surfaces. This includes the use of some compatibilizing surfactants.

The interlayer cations are much less strongly bound than the layer cations and will thus easily exchange with cations from an aqueous solution. This property is a characteristic of the silicate layers and it is characterized by a moderate surface charge known as the cation exchange capacity (CEC). CEC refers to the total quantity of adsorbed cations (e.g., K^+ , Na^+ , Ca^{+2} and Mg^{+2}) at a pH value of 7, and its unit of measurement is mmol/100 g of layered silicate (or MMT). The higher the value of the negative charge of a layered silicate, the stronger is the capacity for hydration, swelling and dispersion. On the contrary, the lower the negative charge, the lower is the capacity of hydration, swelling and dispersion. Measurement of the CEC data and the exchangeable cations of layered silicate are important in evaluating the quality of the minerals and classifying the minerals.

An ion-exchange reaction occurs with the cationic surfactants including primary, secondary, tertiary and quaternary alkyl ammonium cations. Alkyl ammonium cations lower the surface energy of inorganic component and improve the wetting characteristics of the polymer matrix, and result in a larger interlayer spacing as shown in Figure 2.5 (Giannelis 1998). A number of surfactants containing ammonium cations have been studied to modify the clay surfaces. (Gatos, et al. 2004, Gatos and Karger-

Kocsis, 2005). Using surfactant causes an enlargement of the spacing between the clay galleries. This makes the diffusion of polymer molecules into the clay layers favorable.

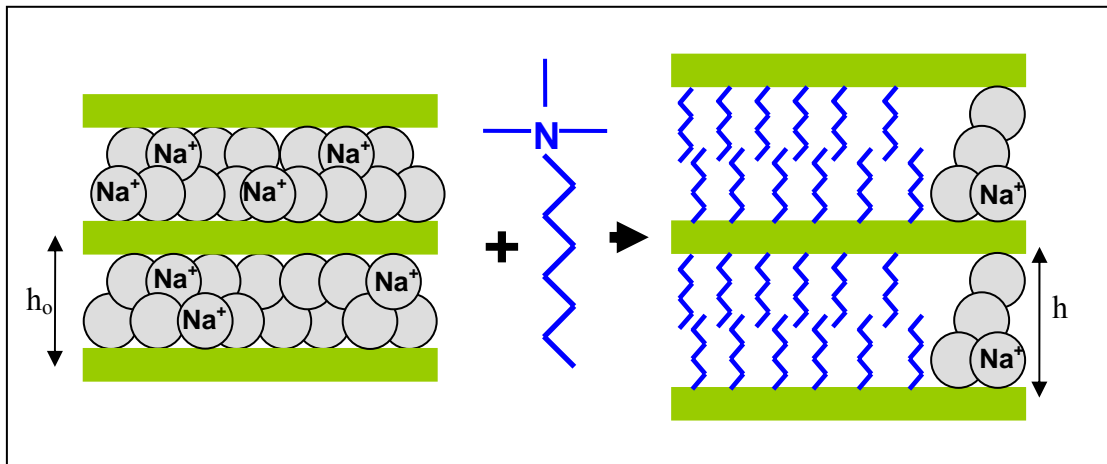


Figure 2.5. Schematic illustration of surface modification of montmorillonite

2.4. Elastomeric Materials

Polymers which are based on olefinic monomers represent a large commercial industry today, including polyethylene and polypropylene in their many forms. These polymers are considered to be thermoplastic, as they have significant levels of crystallinity present at operational temperatures, allowing repeatable forming operations. In these thermoplastic materials, the crystallinity levels are high enough that the material has minimal elastic characteristics. However, copolymers of ethylene and propylene do exhibit a level of strength, and elasticity that allow them to be classified as elastomers. (Morton 1987)

The term elastomer is used to describe vulcanized polymeric materials, whose glass transition is sub-ambient and amongst other properties, has the ability to be extensively deformed and on release of stress, return to its original length. The common characteristics of elastomers are their elasticity, flexibility and toughness. Beyond these common characteristics, each elastomer has its own unique properties, often requiring additives to achieve the appropriate behaviors. Rubber compounding ingredients can be categorized as: vulcanizing or crosslinking agents, processing aids, fillers, antidegradants, plasticizing and other specialty additives (Mohammad and Simon 2006).

The rubbers in the marketplace are of two main types: crosslinking systems and thermoplastic elastomers. Most of commonly used rubbers are polymeric materials with

long chains, which are chemically crosslinked during the curing process. This type of elastomer can not be reshaped, softened, melted or reprocessed by subsequent reheating, once formed. Thermoplastic elastomers, on the other hand, are rubbers which act at room temperature in a manner similar to crosslinked materials but are copolymers, with one phase being rubbery and other crystallizable. These elastomers are generally hydrocarbon based polymers consisting of carbon and hydrogen atoms, although some are polar and may contain other moieties (Dick and Anicelli 2001). They include styrene-butadiene rubber, butyl rubber, polybutadiene rubber, ethylene propylene rubber and polyisoprene rubber, both natural and synthetic.

2.4.1. Ethylene Propylene Diene Rubber (EPDM)

EPDM is one of the most widely used “specialty” elastomers, with a variety of applications as single ply roofing, automotive parts, wire and cable covers, and in other goods that require heat and weather resistance (Morton 1987).

Ethylene-propylene rubber (EPDM) was first introduced in the United States in limited commercial quantities in 1962. Though commercial production began only in 1963, EPDM rubber is now the fastest growing elastomer (Morton 1987). The designation EPDM applies to the simple copolymer of ethylene, propylene and a third comonomer diene which introduces unsaturation into the molecule [‘E’ for ethylene, ‘P’ for propylene, ‘D’ for diene and ‘M’ for the polymethylene $-(CH_2)_x-$].

In Figure 2.6, the structure of ethylene, propylene and the regular, alternating amorphous copolymer of ethylene, propylene are represented.



Figure 2.6. Structure of (a)ethylene, (b)propylene and (c)copolymer of ethylene and propylene (Source: Dick and Anicelli, 2001)

Because of the saturated nature of this polymer molecule (EPM), the normal type of sulfur curatives cannot be employed for vulcanization. Peroxide cure in the presence or absence of a coagent are used instead. Since these cures are expensive and difficult to handle on standard rubber equipment, EPDM polymers were developed and

are now more widely used (Mohammad and Simon 2006). To introduce an unsaturated site suitable for crosslinking, a non-conjugated diene monomer such as ethylidene norbornene, 1,4 hexadiene or dicyclopentadiene, is employed to produce EPDM.

The dienes are so structured that only one of the double bonds will polymerize and the unreacted double bond acts as a site for sulfur crosslinking. This latter unsaturation is also so designed that it does not become part of the polymer backbone but a side group. As a consequence, the terpolymer retains the excellent ozone resistance that the copolymer possesses (Morton 1987). The main desirable properties of EPDM are:

- Aging and ozone resistance of EPDM compounds is excellent
- EPDM compounds have a low temperature flexibility compared with that of natural rubber compounds
- High and excellent level of resistance to chemicals (polar solvents)
- EPDM's non-polarity gives it excellent electrical insulation properties (Dick and Anicelli 2001)
- The heat resistance of EPDM compounds is much better than that of the other rubber types. (Morton 1987)

2.4.1.1. Ethylene-Propylene Composition

The contents of ethylene-propylene elastomers are generally reported as weight-percent ethylene and vary from 80 to 40%. Therefore, generally there is a greater amount of ethylene than propylene. The monomers are randomly distributed, resulting in amorphous type copolymers. As the ethylene content increases, the polymer crystallinity increases. Since crystallinity tends to increase with decrease in temperature, it is appropriate to store high ethylene terpolymers under sufficient warmth to minimize dispersion problems (Dick and Anicelli 2001).

Typically, EPDM polymers are classified as either semi-crystalline or amorphous. Semicrystalline grades generally have ethylene contents of 62 wt.% or greater, while amorphous grades generally have ethylene contents of less than 62 wt.%. Amorphous grades, which have minimal crystallinity, are more flexible at low temperatures, lower hardness, and more elastic. Semicrystalline grades, on the other hand, have several properties that are directly attributable to their crystallinity levels. The higher ethylene-containing polymers exhibit higher tensile strength and modulus,

higher hardness, they can be more highly loaded with fillers/oil, can be more readily pelletized, and possess better extrusion properties. The disadvantage of the higher ethylene contents, is their poorer mill processing behavior at lower temperatures, inferior low-temperature properties, and their difficulty in being mixed (Dick and Anicelli 2001, Morton 1987).

2.4.1.2. Diene Content

In EPDM, as opposed to EPDM, a third monomer is incorporated to add unsaturation to the polymer. These are typically non-conjugated dienes. The unsaturation allows the use of sulfur crosslinking. Three different monomers are used commercially for this purpose. The most common is ethylidene norbornene (ENB), and the two other types are dicyclopentadiene (DCDP) and 1,4-hexadiene (HD) (Vara and Laird). The chemical structures of these three diene type are represented in Figure 2.7. Even though all three introduce unsaturation into the EPDM backbone as vulcanization sites, they impart varying characteristics to the elastomers because of their different structure (Morton 1987).

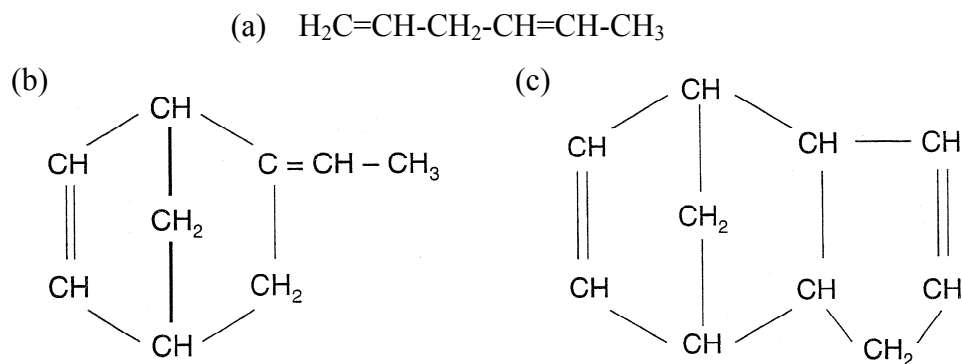


Figure 2. 7. Commercially used diene containing monomers: (a) 1,4 hexadiene, (b) ethylidene norbornene (ENB) and (c) dicyclopentadiene (DCDP) (Source: Morton, 1987)

Ethylidene Norbornene (ENB): ENB is most widely used termonomer employed even though it is most expensive, the reasons being that it is the most readily incorporation during copolymerization and the double bond introduced has the greatest activity for sulfur vulcanization. This activity is also of such a nature that EPDM's containing ENB have the greatest tendency to be occurred with diene elastomers.

Another unique characteristic of this monomer is that it makes it possible to prepare linear as well as branched polymers by varying the conditions under which the polymers are synthesized. Branching has an important role in establishing the rheological properties of a polymer. Under proper control, it can introduce properties to the EPDM that are beneficial in certain applications.

1,4 Hexadiene (1,4 HD): Polymers containing 1,4 HD exhibit a slower cure rate than ENB but possess certain properties that are superior. One such property is its excellent heat characteristic. Such polymers exhibit a good balance of chain scission and crosslinking reactions. Polymers prepared with 1,4 HD are normally linear in structure and possess excellent processing characteristics.

Dicyclopentadiene (DCDP): The main advantages of DCDP are its low cost and relative ease of incorporation, in which it is similar to ENB. Of the three monomers, it has the slowest cure rate. All polymers prepared with it are branched as a result of the slight polymerizability of its second double bond.

In general, several comparisons can be made between the different dienes containing monomers. The fastest cure rates are achieved with ENB, followed by HD and DCDP. Actual rates vary greatly depending on the cure systems used. When diene is added, it is typically between 0.5 wt.% and approximately 12 wt.%. A minimum 2 wt.% diene is required for an effective sulfur cure. Vulcanization processes that utilize batch cures typically use polymers containing 2 to 6 wt.% diene. Continuous cure lines require faster cure rates; therefore, diene levels greater than 6 wt.% are preferred.

2.4.1.3. Crosslinking (Vulcanization) Systems

Vulcanization (curing) is a chemical process designed to reduce the effects of heat or solvents on the properties of a rubber compound and to obtain useful mechanical properties (Dick and Anicelli 2001). The versatile properties of rubbers result from their low glass transition temperatures (T_g) and the ability to increase this property by various types of crosslinking or vulcanization (or curing). During this process, the long chains of the rubber molecules become crosslinked by reactions with the vulcanization agent to form three-dimensional structures, as shown in Figure 2.8. This reaction transforms the soft, weak plastic-like material into a strong elastic product. Sulfur and peroxide, respectively, are the most widely used crosslinking agents (Morton 1987).

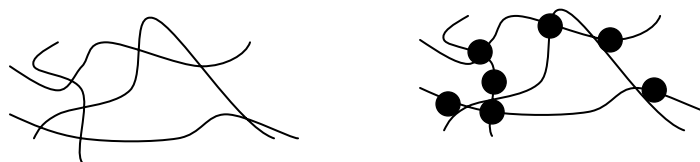


Figure 2.8. Crosslinking process

Before the discovery of vulcanization with sulfur by Charles Goodyear in 1839, John Hancock manufactured waterproof garments, gloves, shoes and boots with just raw natural rubber. These rubber products suffered severely from poor physical properties, poor resistance to light and swelling in liquids and sensitivity to the extreme temperatures. The products became stiff when it was cold and sticky when it was hot. Goodyear's and subsequently Hancock's method of heating rubber and sulfur together resulted in the rubber compound whose sulfur-rubber ratio is 8/100 (by weight) with improved physical properties. This compound was vulcanized for five hours at 140°C. In addition, the product remained stable over a wide range of temperatures and was more resistant to swelling in liquids. However, the aging properties were poor. The shortcomings of using sulfur alone as a vulcanizing agent were recognized early by Goodyear and others, and the search started for additional materials to enhance the number of inorganic oxides such as zinc oxide were tested that followed and did result in shorter cure times, but provided little improvement in the physical properties. The maximum physical properties of this compound were developed in only three hours at 140°C.

The next important discovery in the history of compounding was made by Onslager who, in 1906, found that aniline accelerated the vulcanization process. Aniline is now regarded as the original accelerator. It was found that the reaction of aniline with carbon disulfide yielded an even more powerful accelerator, thiocarbanilide, which was much less toxic and therefore more acceptable than aniline. This combination of zinc oxide and thiocarbanilide reduced the sulfur level, improved significantly the aging properties, and further shortened the vulcanization time. As a result of this success, many trials with derivatives of thiocarbanilide were conducted, and in 1921, mercaptobenzothiazole (MBT) was introduced to become the first really scorch safe accelerator offering many advantages in compounding.

Before the foundations for modern compounding were final, one more important discovery was made concerning the part played by fatty acid constituent in the non-

rubber hydrocarbon portions of natural rubber further activated the vulcanization process with organic accelerators. The addition of stearic acid or similar products therefore became standard practice as a precaution against possible deficiencies in the raw rubber. This compound as listed in Table 2.2 cures in 20 minutes at 140°C and provides vulcanizates with a good balance of processing, curing and physical properties.

Table 2.2. The additives of natural rubber

Natural rubber	100 parts
Sulfur	3 parts
Zinc Oxide	5 parts
Stearic Acid	1 parts
MBT	1 parts

2.4.1.3.1. Sulfur Vulcanization

Sulfur is the most widely used vulcanizing agent in conjunction with activators and organic accelerators. It is a very complex reaction and involves activators for the breakage of the sulfur ring (S_8) and accelerators for the formation of sulfur intermediates, which facilitate sulfur-to-double bond crosslinking as shown in Figure 2.9. Sulfur donors are used to replace part or all of the elemental sulfur to improve thermal and oxidative aging resistance. They may also be used to modify curing and processing characteristics. Two chemicals have been developed over the years to function as sulfur donors (alone or in combination with sulfur) tetramethylthiuram disulfide (TMTD) and dithiodimorpholine (DTDM).

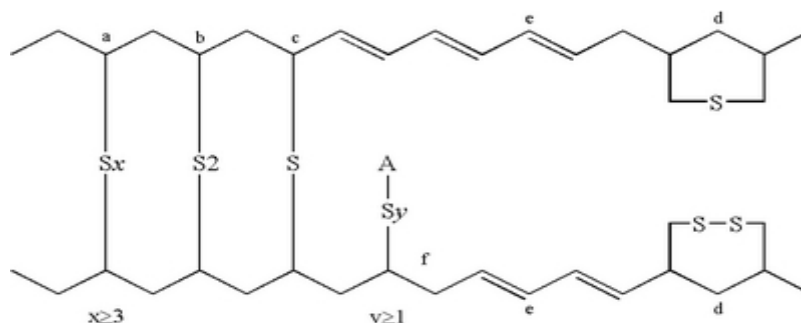


Figure 2.9 Structural features of a sulfur vulcanized rubber

(Source: Morton 1987)

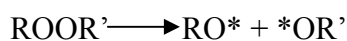
Activators: Activators are both inorganic and organic chemicals used to activate or extract the full potential from the organic accelerators. Zinc oxide is the most widely used inorganic activator while stearic acid is normally the organic activator of choice. Many rubber compounds today incorporate a combination of zinc oxide and stearic acid in sulfur cured compounds.

Accelerators: Accelerators are typically classified as primary or secondary according to their functions. Primary accelerators usually provide considerable scorch delay, medium to fast cure and good modulus development. Secondary accelerators usually produce scorchy, very fast curing stocks. Primary accelerators are thiazoles and sulfenamides. The sulfenamides are reaction products from mercaptobenzothiazole (MBT) or disulfide of mercaptobenzothiazole (MBTS). Typical secondary accelerators are DPG, DOTG, TMTD, TMTM, ZMDC and ZBPD. The secondary accelerators are seldom used alone, but generally are found in combination with primary accelerators to gain faster cures (Morton 1987).

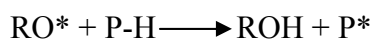
2.4.1.3.2. Peroxide Vulcanization

The saturated rubbers cannot be crosslinked by sulfur and accelerators. Organic peroxides are necessary for the vulcanization of these rubbers. The production of free radicals is the driving force for peroxide crosslinking. These radicals cause an unstable situation and react to allow the electron pair with another. Rubber peroxide crosslinking reaction consists of three basic steps.

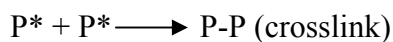
a) Homolytic cleavage: When peroxide is heated to a sufficient temperature, the oxygen-oxygen bond ruptures. The resultant molecular fragments from these ruptures are called radicals, which are highly energetic, reactive species.



b) Hydrogen abstraction: Radicals that have been formed from the peroxide decomposing are reactive toward hydrogen atoms in chains. Hydrogen abstraction is a process where the radical removes a hydrogen atom from another nearby atom. It is a very important step in peroxide curing reaction as it is the mechanism by which radicals are transferred from peroxide molecular fragments to the rubber backbone.



c) Radical coupling (formation of crosslinking): Elastomer radicals are highly reactive species and when two of these radicals come in contact, the unpaired electrons will couple and form a covalent bond or crosslink between the elastomer chains.



The incorporated additives can also affect the peroxide crosslinking reaction because of the ability of the radicals to react with many of the functional groups of these additives.

2.5. Properties of EPDM/Layered Clay Nanocomposites

Ethylene propylene diene rubber has been one of the main industrial rubbers to be investigated with organomodified layered silicates to study the effects of nanoreinforcement on properties. The state of the interface is very important for preparation of composite materials. In EPDM/clay composites a stage of stress exists between the two phases. Such an interface affects the mechanical properties of the composites. Applying a coupling agent for surface modification of clay which reduces the surface energy can improve the interface combination of EPDM/clay composites. When the composite is subjected to external forces, the elastic coating by surfactants will soften the significant changes of stress between two phases. Therefore, the modified clay will reinforce the EPDM as a consequence of the increased compatibility between EPDM and clay.

Besides the structure and the surface properties of clay, the particle size also has an influence on reinforcement of rubber. Fillers of small size can be easily dispersed uniformly in the rubber matrix. They provide a large contact area with EPDM and have a strong reinforcing effect.

2.5.1. Microstructural Properties of EPDM/Layered Clay Nanocomposites

The surfactant to modify the clay, use of MAgEPDM and clay content are the some parameters affected the microstructure of EPDM nanocomposites. The structure of nanocomposites has typically been established using X-Ray diffraction analysis and transmission electron micrographic (TEM).

The key to achieving an exfoliated EPDM/clay nanocomposite is first to use the right surfactant to expand the clay galleries. Different surfactants having different ammonium cations were investigated by Zheng, et al. (Zheng, et al. 2004) and Gatos and Karger-Kocsis (Gatos and Karger-Kocsis 2005). According to the XRD and TEM results of Zheng et.al., MMT modified with trimethyloctadecylamine and dimethylbenzyloctadecylamine existed in the form of an intercalated structure while MMT modified with methylbis(2-hydroxyethyl)cocoalkylamine was fully exfoliated in the EPDM matrix. Gatos and Karger-Kocsis compared the primary and quaternary amine (octadecylamine and octadecyltrimethylamine, respectively) intercalated MMT. They observed that increasing polarity of the EPDM favors the intercalation/exfoliation of the organoclay irrespective to the type of its surfactant (primary or quaternary). Exfoliation is likely favored by the possible interaction of the MAgEPDM.

To observe the effect of MAgEPDM as a compatibilizer, the composites with and without MAgEPDM were prepared by Ahmadi, et al. (Ahmadi, et al. 2005). As a result, MAgEPDM increased the interlayer spacing of the clay as well as its compatibility with polymer, so the clay galleries could be easily intercalated with the EPDM (Figure 2.10). The results were confirmed by Transmission electron micrographs shown in Figure 2.11.

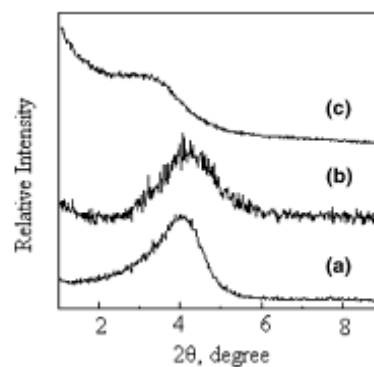


Figure 2.10. XRD patterns of: (a) organoclay (2 g), (b) EPDM (100 phr) + organoclay (3 phr) and (c) MAH-g EPDM (100 phr) + organoclay (3 phr) (Source: Ahmadi, et al. 2005)

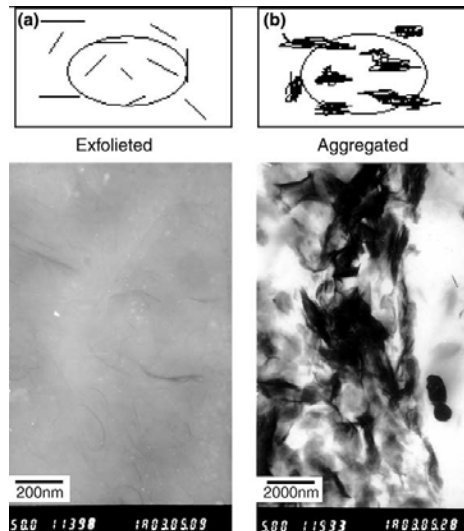


Figure 2.11. Transmission electron micrographs of (a) EPDM (100 phr) + organoclay (3 phr) and (b) MAH-g EPDM (100 phr) + organoclay (3 phr) (Source: Ahmadi, et al. 2005)

The microstructure of EPDM nanocomposites could also change during the vulcanization process. Hence, when the vulcanization accelerators of EPDM/clay nanocomposites, thiourea (NPV/C), 2-mercaptobenzothiazole (M), N-cyclohexyl-2-sulfonamide (CZ), tetramethylthiuram monosulfide (TS) and zinc dimethyldithiocarbamate (PZ) were compared, it was observed that EPDM/clay composites prepared by tetramethylthiuram monosulfide (TS) and zinc dimethyldithiocarbamate (PZ) were exfoliated and dispersed to the monolayers. However, when thiourea (NPV/C), 2-mercaptobenzothiazole (M) and N-cyclohexyl-2-sulfonamide (CZ) were used as accelerators, the dispersibility of clays in EPDM was insufficient. The XRD patterns are shown in Figure 2.12.

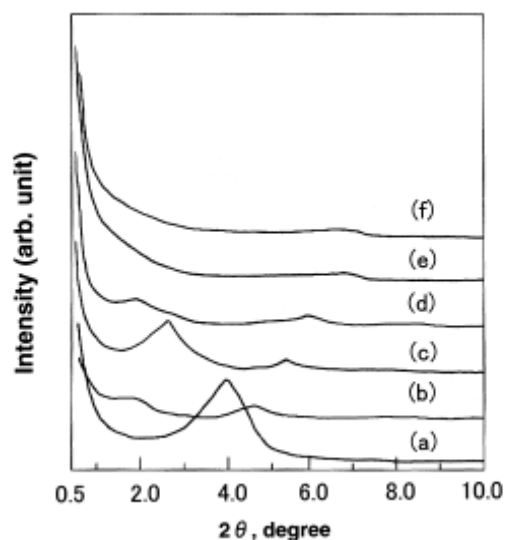


Figure 2.12. XRD patterns of a) octadecylammonium modified MMT and b-f) EPDM/clay nanocomposites used five types of vulcanization accelerators: b) thiourea (NPV/C), c) 2-mercaptobenzothiazole(MBT), d) N-cyclohexyl-2 sulfonamide(CZ), e)tetra- methylthiuram monosulfide (TS) and f) zinc dimethyldithiocarbamate (PZ) (Source: Ahmadi, et al. 2005)

The structure of EPDM is another parameter that affects the morphology of the EPDM/clay nanocomposites. In this respect, Ma, et al. (Ma, et al. 2005) investigated the influence of the ethylene content (52, 67, 70 %) in EPDM on the morphology of the nanocomposite. As a filler, montmorillonite modified with octadecyltrimethyl ammonium was used. As a result, a little influence of ethylene content in EPDM matrix on the morphology of the nanocomposite was observed.

2.5.2. Mechanical Properties of EPDM/Layered Clay Nanocomposites

The tensile test is a destructive test considered to be one of the oldest tests performed in the rubber industry. Tensile strength is the amount of required force to break a material in tension, conducted by stretching a sample in a test machine until it breaks and measured in units of force per unit of area. The mechanical properties of nanocomposites are directly proportional with the dispersion of clay in polymer matrix.

Usuki, et al. (Usuki, et al. 2001) investigated the effect of five different accelerators on the nanocomposites of EPDM/layered silicate. The layered silicate, montmorillonite, was modified by octadecylamine surfactant. Thiourea (NPV/C), 2-

mercaptobenzothiazole (MBT), N-cyclohexyl-2-sulfonamide (CZ), tetramethylthiuram monosulfide (TS) and zinc dimethyldithiocarbamate (PZ) were compared as vulcanization accelerators. As a result, they found that the nanocomposites prepared successfully by thiuram (TS) and dithiocarbamate (PZ) type compounds. The tensile strength of nanocomposite containing 4 wt.% OMMT was 2 times higher than that of neat EPDM. In addition, the gas permeability of EPDM/clay nanocomposites decreased 30% as compared with neat EPDM.

Different processing conditions (at temperature of 25 and 90°C and rotor speed of 34, 68, 136 rpm) were investigated by Zheng, et al. (Zheng, et al. 2004). Methylbis(2-hydroxyethyl)cocoalkylamine was used as a surfactant to modify the layered silicate. The tensile strength and elongation at break of the EPDM composites increased with increasing rotor speed but modulus at 100% and 300% extension and tear strength of the composites were only slightly affected by increasing rotor speed. As a result, they found that to obtain composites with good mechanical properties, the mixing temperature was fixed at 90°C and the rotor speed at 136 rpm. For effective dispersion of clay in EPDM matrix, high mechanical shear stress produced by the high rotor speed play an important role. The increase in temperature was decreased the viscosity of the matrix which in turn facilitated the breakup process of the OMMT agglomerates and resulting in relatively fine dispersion of the OMMT and improvement of the mechanical properties.

To observe the effect of MAgEPDM as a compatibilizer, the composites with and without MAgEPDM were prepared by Ahmadi, et al. (Ahmadi, et al. 2005). They found that the tensile strength, modulus and hardness of EPDM/organoclay nanocomposites containing MAgEPDM substantially were increased relative to EPDM/organoclay composites without MAgEPDM but elongation at break is decreased.

The direct and indirect methods of melt-blending were investigated by Ahmadi, et al. (Ahmadi, et al. 2005). In direct method, MAgEPDM and organoclay were melt-mixed for 15 min then EPDM and this compound were melt-blended for 15 min. In indirect method, EPDM, MAgEPDM and organoclay were melt-blended in one stage for 15 min. The mechanical properties of nanocomposites obtained by two different methods are almost the same; however the direct method has lower cost and is industrially more practical.

Gatos, et al. (Gatos, et al. 2004) were also investigated the MAgEPDM effect on the mechanical properties of EPDM/clay nanocomposites. As vulcanization accelerators, N-cyclohexyl-2-benzothiazole (CBS), 2-mercaptobenzothiazole (MBT) and zinc diethyldithiazole (ZDEC) were used. The montmorillonite was modified with octadecylamine. Separately, the mixer type (open mill and internal mixer) and mixing temperature (at room temperature and 100°C) were studied. In Table 2.3, the mechanical test results were shown for EPDM/clay nanocomposites prepared by ZDEC accelerator which was given the best mechanical result. As seen from this table, while the processing conditions have a limited effect on the mechanical properties, use of MAgEPDM compatibilizer resulted in markedly higher values of tensile strength and stiffness.

Table 2.3. Mechanical properties of EPDM/organoclay (10 phr) compounds, prepared under different conditions with and without MAgEPDM compatibilizer (Gatos , et al. 2004)

Properties	Processing conditions							
	Open mill				Internal mixer			
	Room temperature		100°C		Room temperature		100°C	
	EPDM	EPDM-MA50 %	EPDM	EPDM-MA50 %	EPDM	EPDM-MA50 %	EPDM	EPDM-MA50 %
Tensile strength (MPa)	3.9	6.6	5.2	8.1	4.9	10.5	7.1	14.9
Tensile modulus (MPa)								
100 % Elongation	1.5	2.0	1.6	2.7	1.5	3.9	1.6	5.4
200 % Elongation	2.3	3.3	2.3	4.6	2.0	7.3	2.3	9.3
300 % Elongation	3.0	4.9	2.9	6.9	2.6	9.9	3.0	12.1
Elongation at break (%)	380	395	495	360	520	321	645	403

When the influence of ethylene content in EPDM matrix on the mechanical properties of EPDM/clay nanocomposites were examined (Ma , et al. 2005), it was found that the tensile strength of EPDM/clay nanocomposites was increased with ethylene content.

2.5.3. Thermal Properties of EPDM/Layered Clay Nanocomposites

The decomposition temperatures of montmorillonite and modified montmorillonite were investigated by Zheng , et al. (Zheng , et al. 2003). It was revealed that the organomodified montmorillonite exhibits lower weight loss than unmodified montmorillonite between 45-100°C corresponding to the removal of water form interlayers. Between 100-600°C, the weight losses of OMMT was found to be

greater than MMT corresponding to decomposition of hydrogen bonded water molecules and some of the OH groups from tetrahedral sheets. They also investigated the effect of MAgEPDM on the dynamic storage moduli of the composites. The dynamic storage moduli of the composites containing MAgEPDM were found to be higher than those of composites without MAgEPDM. This indicates the strong interfacial interactions in the composites containing MAgEPDM.

Mousa (Mousa 2006) studied the effects of octadecyltrimethylammonium modified montmorillonite concentration on the thermal properties of EPDM/clay nanocomposites. It was found that the heat of vulcanization reaction was increased with increase in organoclay content as demonstrated in Figure 2.13. It is inferred that organoclay is not only a filler but also could act as a curing agent. It was also found that the increase in organoclay content increases the thermal stability of the composites based on TGA results as shown in Figure 2.14. It was attributed to the nano organoclay dispersion and improved interaction between the organoclay and elastomeric matrix.

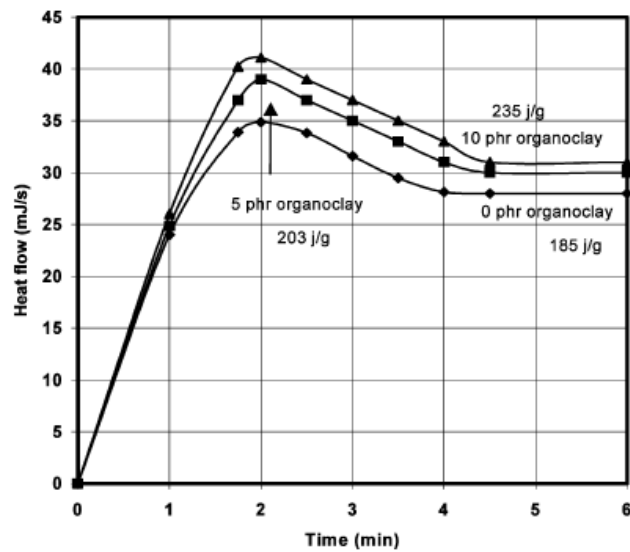


Figure 2.13. Isothermal DSC thermograms for EPDM composites with various organoclay loading (Source: Mousa 2006)

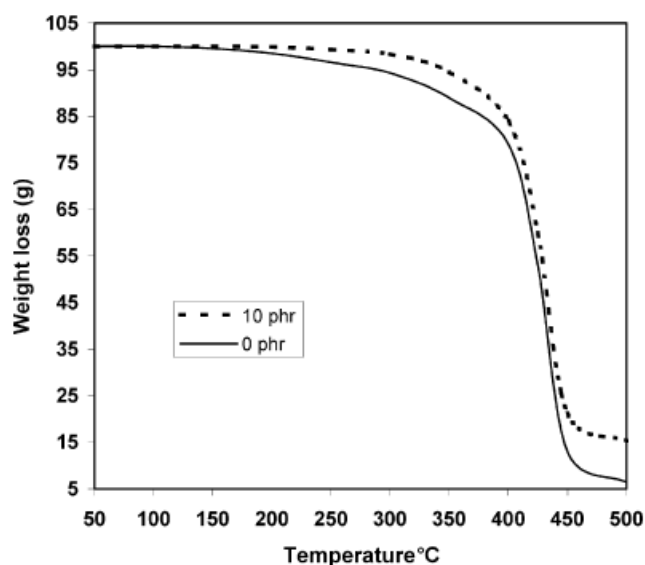


Figure 2.14. TGA thermograms of unfilled EPDM and 10% filled EPDM nanocomposite (Source: Mousa 2006)

Liu, et al. (Liu, et al. 2005) also investigated the clay content effect on the thermal properties of EPDM/clay nanocomposites prepared by a different technique. It was found that resistance to thermal degradation is improved by clay loading. Nanosized MMT layers are able to retard the heat diffusion into EPDM matrix. On the other hand, T_g and storage modulus values increased with the addition of MMT based on DMA results.

The effect of different surfactants on thermomechanical properties of EPDM/clay nanocomposites were investigated by Zheng, et al. (Zheng, et al. 2004). As a result, the storage modulus of the EPDM/ methylbis(2-hydroxyethyl)cocoalkylamine modified montmorillonite nanocomposite was the largest among the other composites. However, the T_g of the composites remained constant as compared to that of neat EPDM. On the other hand, Ahmadi, et al. (Ahmadi, et al. 2004) also investigated the thermomechanical properties of the nanocomposites and obtained that the clay addition shifted the T_g towards higher temperatures. In addition, the $\tan \delta$ value of EPDM/modified clay nanocomposite was decreased as compared to neat EPDM and EPDM/unmodified clay composites. The lower $\tan \delta$ and the increased storage modulus were explained by maximum adhesion between polymer and layered silicate surface because of nanometer size.

CHAPTER 3

EXPERIMENTAL

3.1. Materials

Na⁺ montmorillonite (MMT) clay particles as a filler and EPDM as the polymer matrix were used to prepare nanocomposites. EPDM had PP content of 28%, oil content of 40% and ENB content of 5.5%. EPDMgMA (with a density of 0.87gr/cm³) was used as compatibilizer and octadecylamine was used as surfactant to modify MMT particles. In addition, sulfur was used as a vulcanizing agent, TMTD (tetramethyl thiuram disulfide) and MBT (mercaptobenzotiazol) were used as accelerators, and zinc oxide and stearic acid were used as activators for vulcanization process. The details of the materials used in this study are given in Table 3.1. The structures of EPDM polymer and octadecylamine are illustrated in Figure 3.1.

Table 3.1. Details of materials used

Material	Supplier	Characteristics
EPDM Trade name, Dutral 4436	Polimeri Europa	Mooney viscosity ML ₍₁₊₄₎ (125°C)= 43
EPDMgMA Trade name, Fusabond N MF416D	Dupont	MFI (2800C, 2.16kg)= 23 g/10min
Montmorillonite -K10	Sigma Aldrich	CEC: 120 meq/100 g Size: 0.01-1.0 µm
Octadecylamine (90%)	Sigma Aldrich	Molecular weight, M _w =269.51

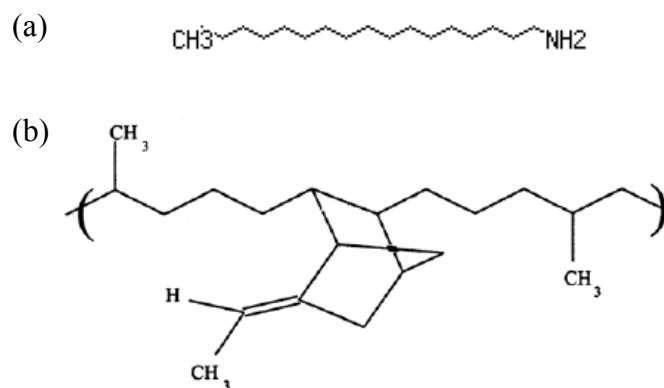


Figure 3.1. Structure of (a) EPDM containing ENB, (b) octadecylamine

3.2. Modification of Clay

Surface modified organophilic Na⁺-montmorillonite (OMMT) was prepared from organophobic pure Na⁺-montmorillonite (MMT) via an ion-exchange reaction in water with alkylammonium surfactant. The surface modification procedure is schematically shown in Figure 3.2. For modification, 40 g Na⁺-MMT was dispersed in 2500 ml of deionized hot water at 80°C by using a homogenizer to obtain a suspension. 15.5 g (57.5 mmol) octadecylamine and 5.75 ml of concentrated HCl were dissolved in 1000 ml of deionized hot water at 80°C. This solution was poured in the MMT–water solution with vigorous stirring by using the homogenizer for 1 h to yield white precipitate. The precipitate was collected on a filter and washed with deionized hot water until chloride anions were not detected with a 0.1 M AgNO₃ solution, and then it was dried in a vacuum oven at 80°C. OMMT was obtained after grinding and screening with a 325-mesh sieve.

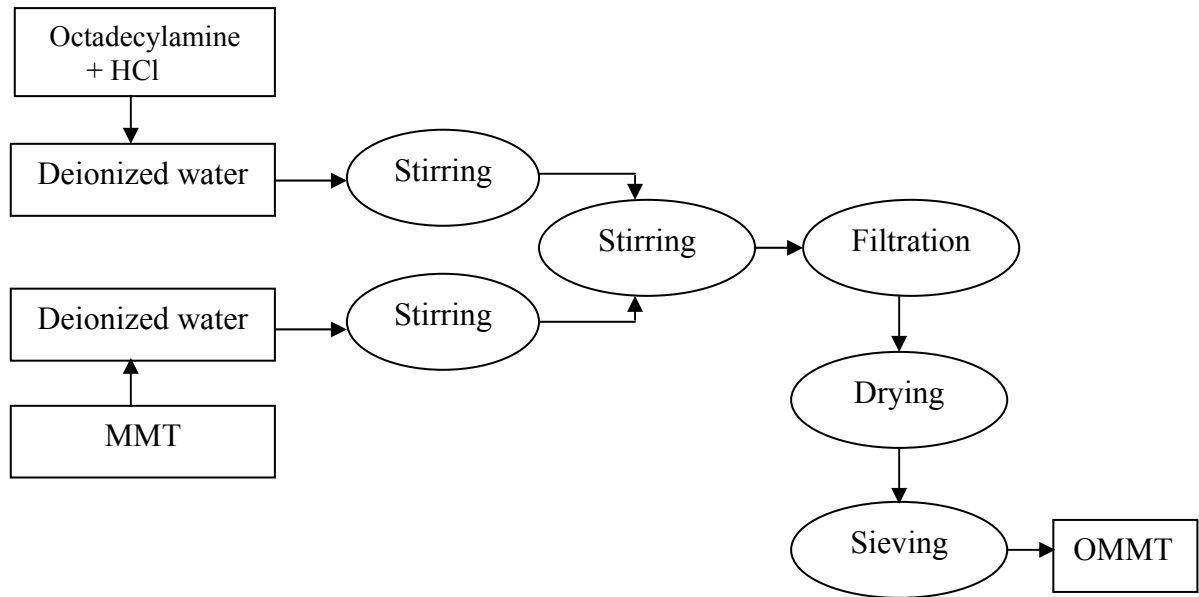


Figure 3.2. Schematic illustration of surface modification of montmorillonite

3.3. Preparation of EPDM/Clay Nanocomposites

EPDM, organoclay (OMMT) and maleic anhydride grafted EPDM oligomer (EPDMgMA) were blended by melt-mixing method in a HAAKE Rheometer RC90 (Haake Co., Germany) as shown in Figure 3.2. The blending temperature of 120 and 150°C, a rotor speed of 60 and 90 rpm and mixing time of 10, 15 and 20 min was selected as selected parameters. The compositions of neat EPDM and EPDM/OMMT nanocomposites are shown in Table 3.3. In the first stage, EPDMgMA was melt-mixed with OMMT using the rheometer to obtain masterbatches. In the second stage, EPDM and the pre-mixture of OMMT/EPDMgMA were melt-blended for 10, 15 and 20 min to prepare the EPDM/OMMT nanocomposites. The EPDM/OMMT blend were sequentially mixed with zinc oxide (5 phr), stearic acid (1 phr), vulcanization accelerator [MBT (0.5 phr) and TMTD (1.5 phr)] and sulphur (1.5 phr) by using a roll mill (Ak Plastic Inc., Turkey) as shown in Figure 3.4 at ambient temperature. Vulcanized EPDM/OMMT was compression molded (140 mm x 140 mm x 2 mm) under a hot press at 160°C for 20 min to obtain rubber sheets. The EPDM/clay nanocomposite production scheme is illustrated in Figure 3.5.



Figure 3.3. Haake Mixer

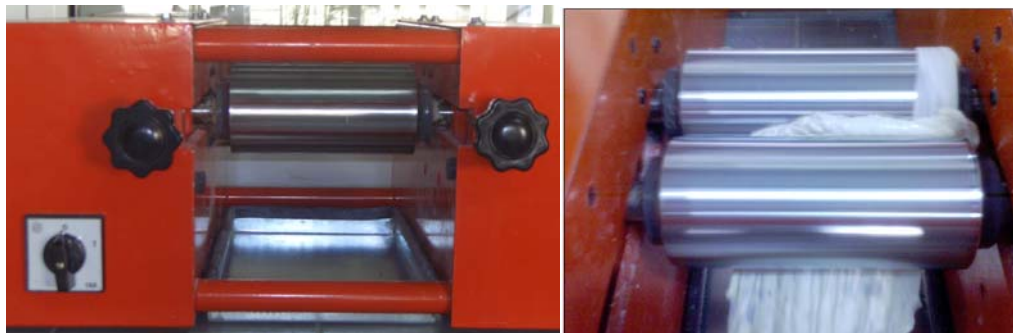


Figure 3.4. Two roll mill

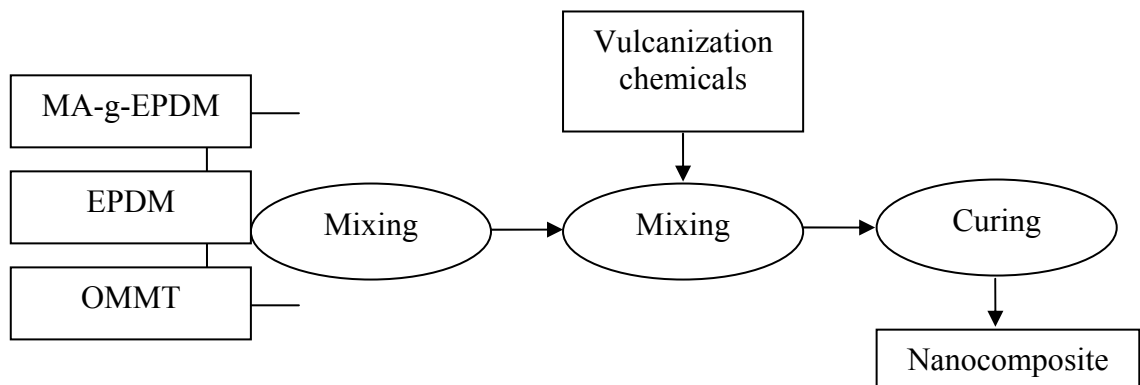


Figure 3.5. Schematic illustration of production of EPDM/clay nanocomposites

Table 3.2. Composition of neat EPDM and EPDM/OMMT nanocomposites

Sample Component (phr)	Neat EPDM	EPDM/ 5wt.% OMMT	EPDM/ 10wt.% OMMT
EPDM	100	100	100
EPDMgMA	20	20	20
Organoclay (OMMT)	-	5	10

3.4. Characterization of Nanocomposites

The nanocomposites of layered clay/EPDM were characterized by performing characterization techniques described below. The effects of the layered clay addition on the microstructural, thermal and mechanical properties of the nanocomposites were investigated in comparison with the properties of EPDM.

3.4.1. Morphological Investigation

3.4.1.1. X-Ray Diffraction (XRD)

To investigate the effect of surface modification on the intercalation of the clay layers XRD technique was employed. The change of basal spacing of MMT after modification with octadecyl ammonium ion and also after mixing with EPDM was studied. XRD was carried out using Bruker AXS D8 with Cu K α radiation at 40 kV and 40 mA. The diffractograms were scanned in 2 θ range from 1° to 10° at a rate of 2°/min. Specimens were cut from vulcanizate sheets perpendicular to the direction of vulcanizate sheet surface.

3.4.1.2. Scanning Electron Microscopy (SEM)

Dispersion of the silicate layers in the polymer matrix was investigated by using SEM (Scanning electron microscopy (Phillips XL-30S FEG-SEM)) from the fractured surface of the tensile samples. All the sample surfaces were gold-coated by a sputtering apparatus before SEM examination. In addition, the elemental analysis on the sample surfaces was performed by Energy Dispersion Spectroscopy (SEM-EDX) attached to SEM equipment.

3.4.1.3. Fourier Transform Infrared Spectroscopy (FTIR)

Fourier Transform Infrared Spectroscopy (Perkin Elmer, Spectrum BX) was used for the identification of the montmorillonite, surfactant octadecylamine and

organically modified montmorillonite over a frequency range from 400 to 4000 cm^{-1} . The samples were prepared as KBr pellets.

3.4.2. Measurement of Mechanical Properties

3.4.2.1. Tensile Test

The tensile mechanical tests were performed using a Zwick Z020 (Ulm, Germany) universal testing machine (Figure 3.6) at a cross-head speed of 200 mm/min based on type II specimens according to DIN 53504 standard. Using the molded sheets obtained from compression mold, five dogbone samples as shown in Figure 3.6 for each compound were cut in the vulcanizate's milled direction. Measurement of the thickness of the samples was done with a precision of 0.01 mm. Three thickness measurements were made for each sample.



Figure 3.6. Photo of tensile test and tensile test specimen

3.4.2.2. Tear Test

The tear strength of the nanocomposites was measured using an Instron-4505 (Instron Inc., United Kingdom) universal testing machine at a crosshead speed of 500 mm/min, in accordance to DIN 53507 standard. At least five specimens from each batch were tested at 23°C. The averages of three thickness measurements were taken.



Figure 3.7. Tear test specimen before and after the tear test

3.4.2.3. Hardness Measurements

The hardness measurements of the EPDM/OMMT nanocomposites were made by using Vickers method. Hardness values of the specimens were measured using a Shore-A durometer (Bariess, Germany) based on DIN 53505 standard. Hardness values of each specimen were measured at five different part of the each sample and the average of them and also the standard deviations were calculated.

3.4.2.4. Aging Test

Neat EPDM and EPDM/OMMT nanocomposites were prepared as tensile test samples as described above. The samples were exposed to detergent (1 wt. %) water at 95°C, for 300 hours. After aging, the mechanical tests based on the procedure explained above were performed to investigate the effect of aging environment on the mechanical properties of the neat EPDM and EPDM/OMMT nanocomposites.



Figure 3.8. The equipment used for aging experiment

3.4.3. Measurement of Thermal Properties

To analyse the weight loss and the reactions of the polymeric structure at different temperatures, thermal analysis were performed. Moreover, the effects of clay addition on the weight loss and phase change were investigated.

3.4.3.1. Differential Scanning Calorimetry (DSC)

DSC measurements were carried out on TA Instruments differential scanning calorimeter model Q10. Samples of 5-6 mg of EPDM/clay nanocomposites were scanned from -100 °C to 100°C under nitrogen atmosphere at a heating rate of 10 °C/min. The glass transition temperature (T_g) was determined by the midpoint method.



Figure 3.9. DSC equipment

3.4.3.2. Thermogravimetric Analysis (TGA)

Thermogravimetric analysis is a technique which analyze the weight alteration as a result of heat, in other words, it determine the degradation temperature of the sample. The weight loss measurements of the samples were performed on Perkin Elmer termogarvimetric analyzer. The experiments were carried out from 25°C to 200°C.

3.4.3.3. Dynamic Mechanical Analysis (DMA)

Dynamic mechanical analysis (DMA) was recorded on tensile mode with an amplitude of 0.15% at a frequency of 10 Hz using a Pyris Diamond device of Perkin Elmer. By using DMA, the storage modulus (E'), mechanical loss factor ($\tan \delta$) were measured in the temperature range from -100 to 120°C at a heating rate of 2°C/min.



Figure 3.10. DMA equipment

CHAPTER 4

RESULTS AND DISCUSSION

4.1. Investigation of Intercalation and Dispersion of Clay Layers

Pristine MMT and organically modified MMT used in the nanocomposite structures were characterized by X-Ray Diffraction to determine the intercalation of the layered clays by measuring the d-spacing of the silicate layers within the clays. Also, XRD was used to characterize the degree of exfoliation of the organoclay in the rubber matrices.

Figure 4.1 illustrates the XRD patterns of pristine clay (MMT) and organically modified clay (OMMT). Unmodified clay (MMT) exhibits a single peak at 2θ of 6, which corresponds to a basal spacing of 14.6 Å, while the modified clay have two different characteristic peaks at 2θ of 2.9 and 5.4, which correspond to a basal spacing of 30.9 and 16.3 Å, respectively. This corresponds to a successful organic modification of MMT. During organic modification, the long alkyl chains are intercalated into the galleries of MMT through an ion exchange reaction between Na^+ and the alkyl ammonium cations. Improved intercalation of the long alkyl chains leads to the larger interlayer spacing and the delamination of the clay mineral is enhanced within the polymer matrix. The XRD pattern for neat EPDM is given in Figure 4.2. Neat EPDM shows a characteristic peaks at $2\theta = 9^\circ, 18.7^\circ, 24.7^\circ, 28.4^\circ, 31.6^\circ, 34.2^\circ, 36^\circ, 47.4^\circ, 56.4^\circ, 62.6^\circ, 66^\circ, 67.7^\circ$ and 69° . As seen in the figure, neat EPDM does not exhibit any peak similar to those of MMT.

To investigate the effects of the blending time on the intercalation of clay in EPDM matrix, the blending time and OMMT content were altered during nanocomposite preparation. In this case, the blending speed and temperature were fixed at 90 rpm and 150°C. The blends were compounded by Haake internal mixer for 10, 15 and 20 min. Figure 4.3 shows the effect of blending time on the microstructure of the EPDM/OMMT nanocomposites.

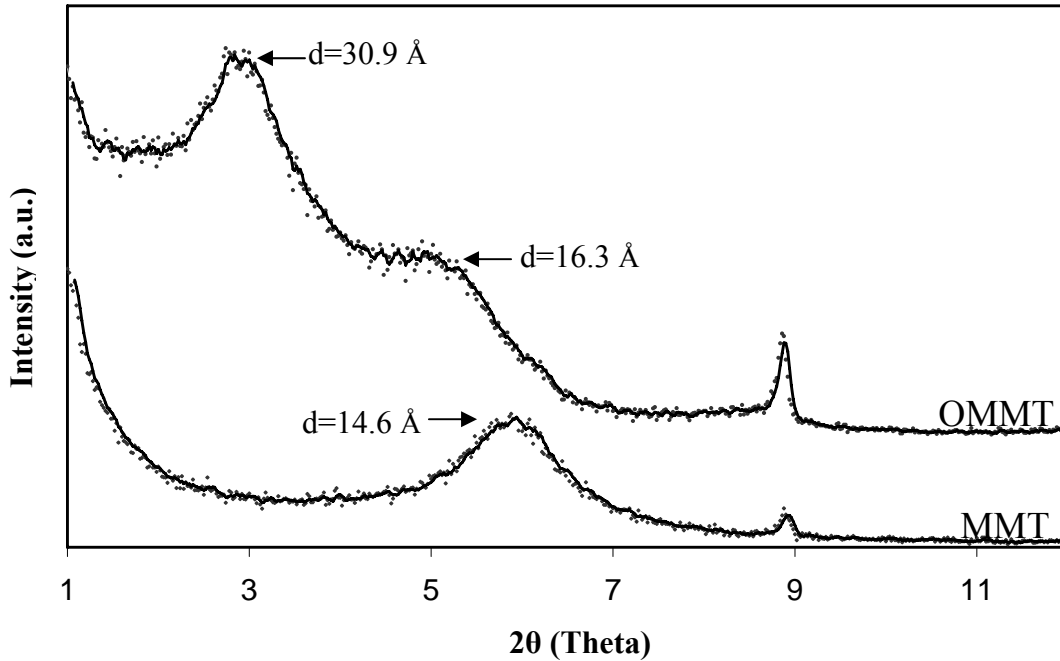


Figure 4. 1. XRD patterns of Na⁺-montmorillonite and organo modified montmorillonite

It was observed that although some peaks are visible for nanocomposites containing 5 and 10 wt. % of OMMT, by melt-blending for 10 and 15 minutes, a small degree of deintercalation may be suggested due to agglomeration. However, by increasing the blending time to 20 min, broad peaks were observed, which imply the expansion of basal spacing and occurrence of intercalated EPDM chains into the silicate layers, while some of which were evidence for exfoliation into the EPDM matrix. This indicates that the silicate layers had extent of exfoliation and dispersed uniformly in EPDM when the blending time was set to 20 min.

The same tendency was also observed for EPDM/10 wt. % OMMT nanocomposites compounded at different blending times. Blending time of 10, 15 and 20 min was used for nanocomposite preparation. As a result, at 5 and 10 wt. % concentrations, OMMT containing nanocomposites achieved by-melt blending for 20 minutes did not exhibit any peak while the others exhibit a broad peak at about 6.5°. This indicates a fraction of exfoliation of clay layers with the EPDM matrix for blending time of 20 min.

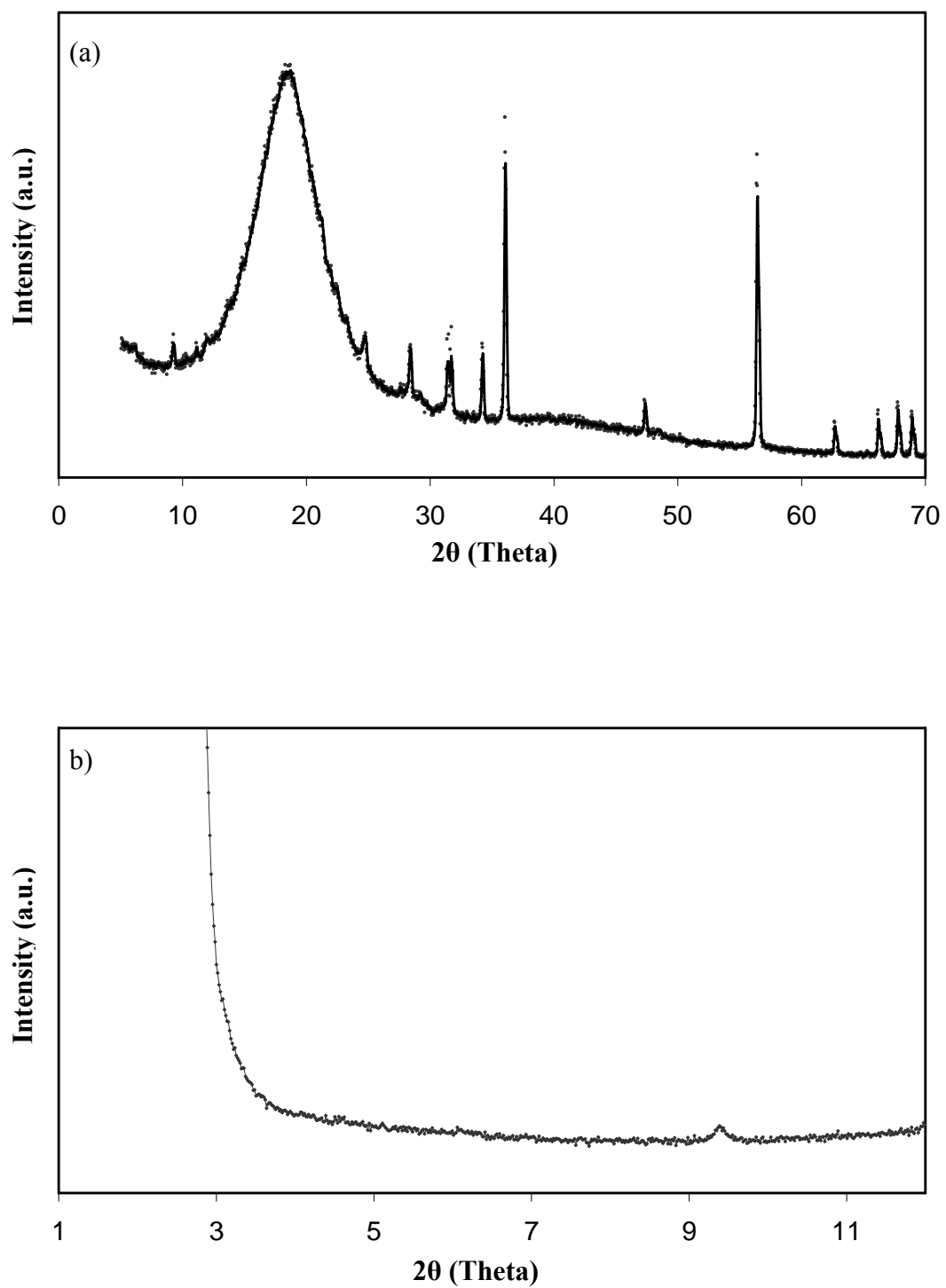


Figure 4. 2. XRD pattern of neat EPDM between a) $2\theta=5-70^\circ$, b) $2\theta=1-12^\circ$

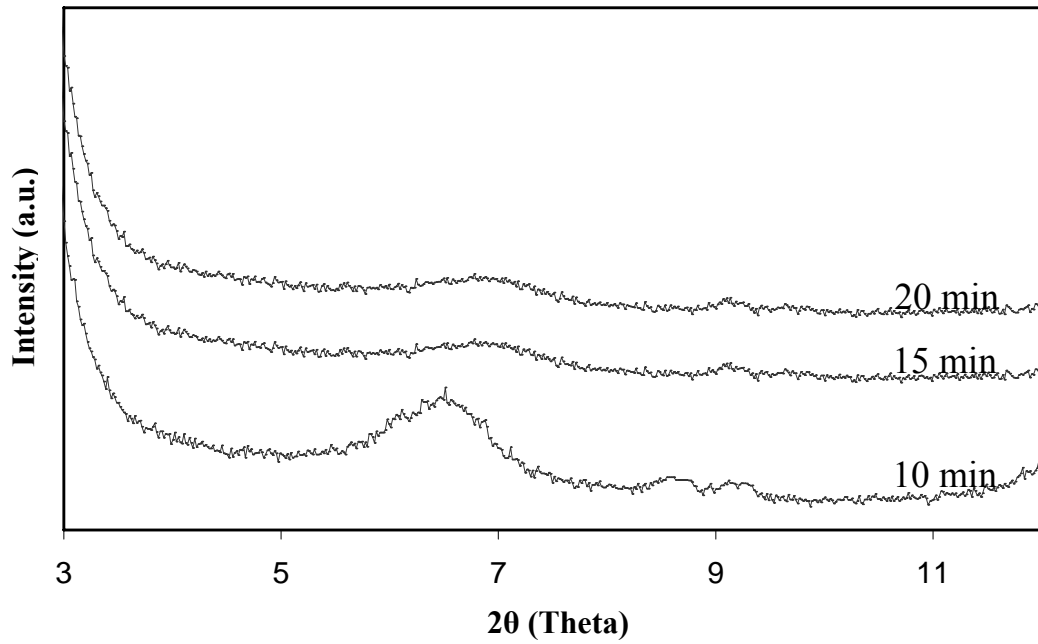


Figure 4. 3. XRD patterns of EPDM/ 5 wt. % OMMT nanocomposites with 10, 15 and 20 min blending time (blending temperature=150°C, blending speed=90 rpm)

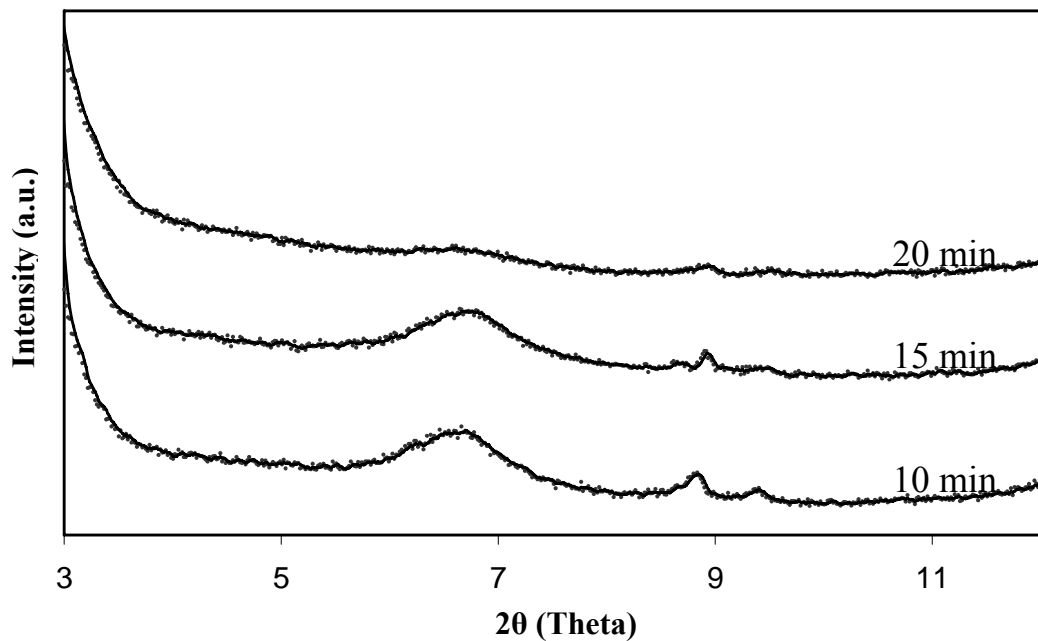


Figure 4. 4. XRD patterns of EPDM/ 10 wt. % OMMT nanocomposites with 10, 15 and 20 min blending time (blending temperature=150°C, blending speed=90 rpm)

To monitor the effect of processing temperature on the properties, nanocomposites containing 5 and 10 wt. % OMMT were prepared at two different

temperatures (120 and 150°C). According to the XRD results, the effect of blending temperature was insignificant on the final microstructure of the nanocomposites containing 5 and 10 wt. % OMMT.

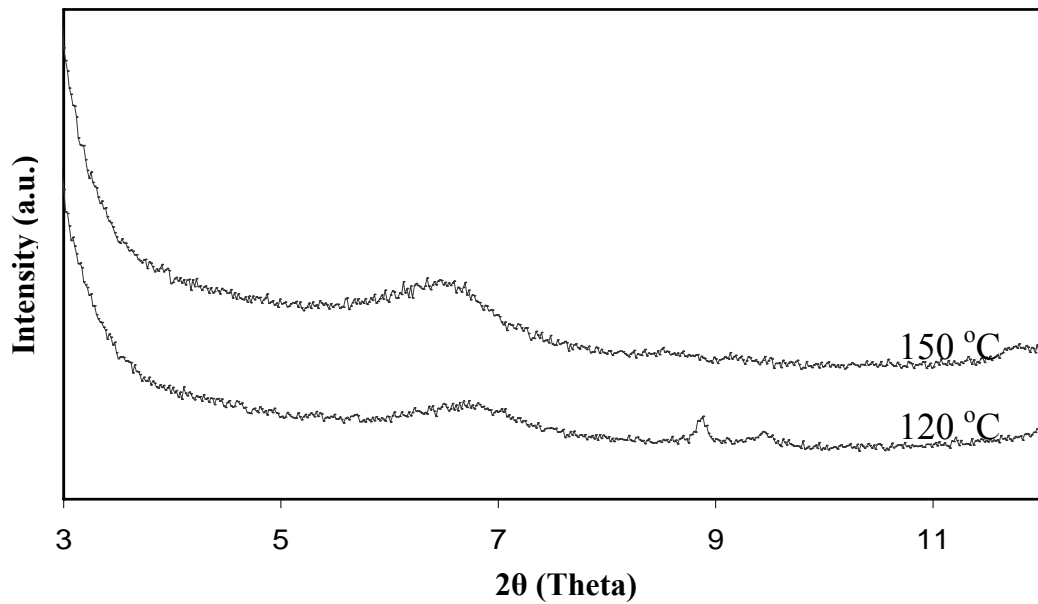


Figure 4. 5. XRD patterns of EPDM/ 5 wt. % OMMT nanocomposites with 120 and 150°C blending temperature (blending time=15 min, blending speed=90 rpm)

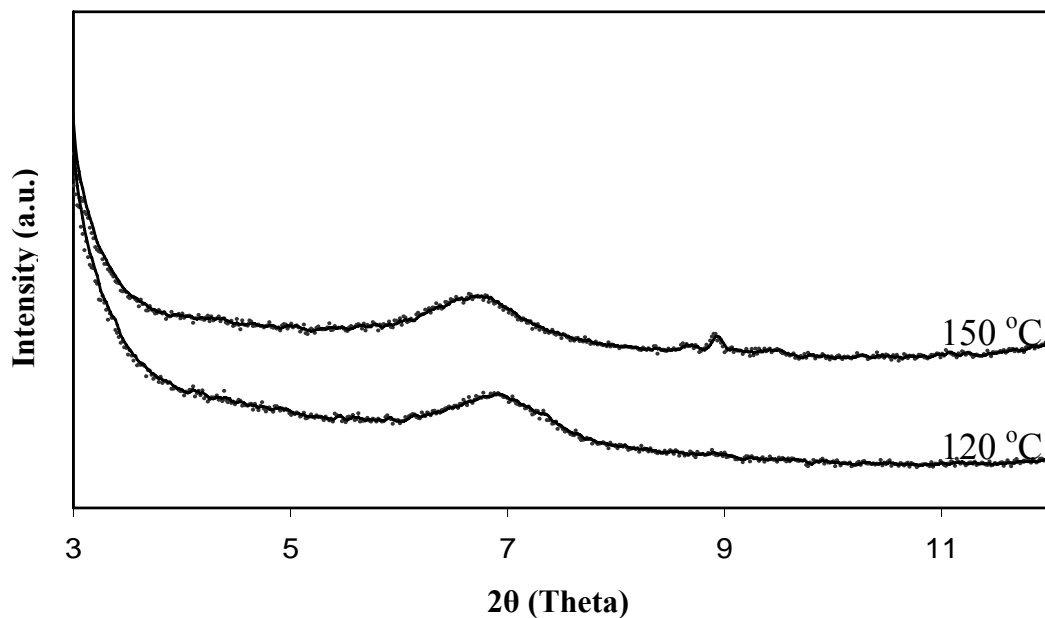


Figure 4. 6. XRD patterns of EPDM/ 10 wt. % OMMT nanocomposites with 120 and 150°C blending temperature (blending time=15 min, blending speed=90 rpm)

The effect of blending speed for the nanocomposite structures was also insignificant due to the degree of observed intercalation. Both compositions of 5 and 10 wt. % EPDM/OMMT systems showed the characteristic peak of MMT at around $2\theta=6.5^\circ$. We can conclude that the increase in blending speed was insufficient to increase the degree of intercalation and exfoliation of clay platelets within the EPDM matrix. However, for EPDM/5 wt. % OMMT nanocomposites, 60 rpm blending speed gave better XRD result.

In summary, based on XRD investigations, it was found that the surface modification of the clay particulates results in intercalation of clay layers. It was also observed the intercalation of clay layers within the EPDM molecules occurs during blending. The effect of blending time was found to be more significant on the formation of EPDM/OMMT nanocomposite structures than those of the blending temperature and rotor speed.

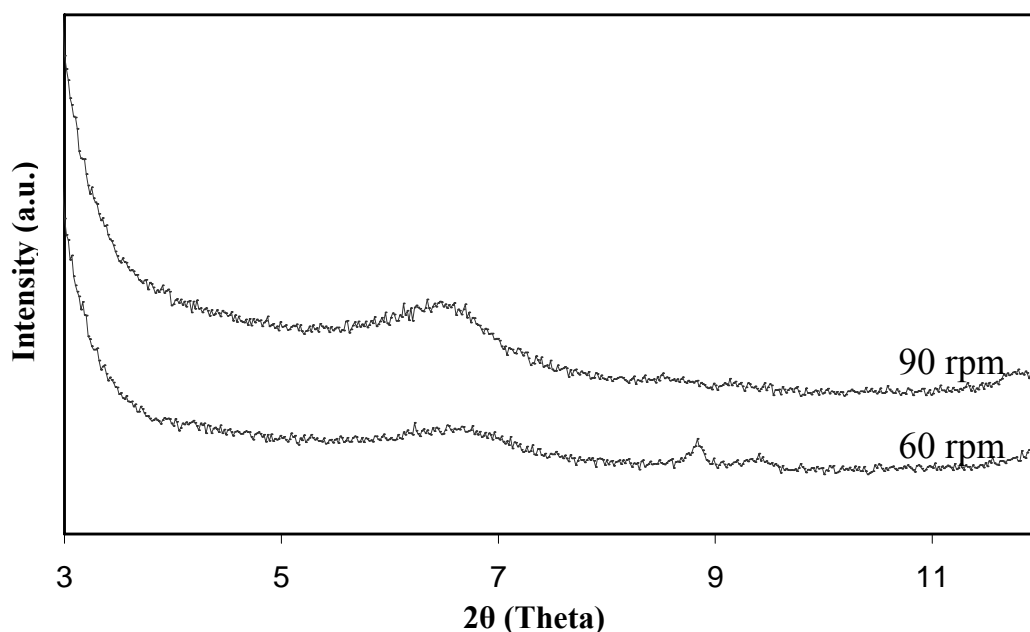


Figure 4. 7. XRD patterns of EPDM/ 5 wt. % OMMT nanocomposites with 60 and 90 rpm blending speed (blending time=15 min, blending temperature=150°C)

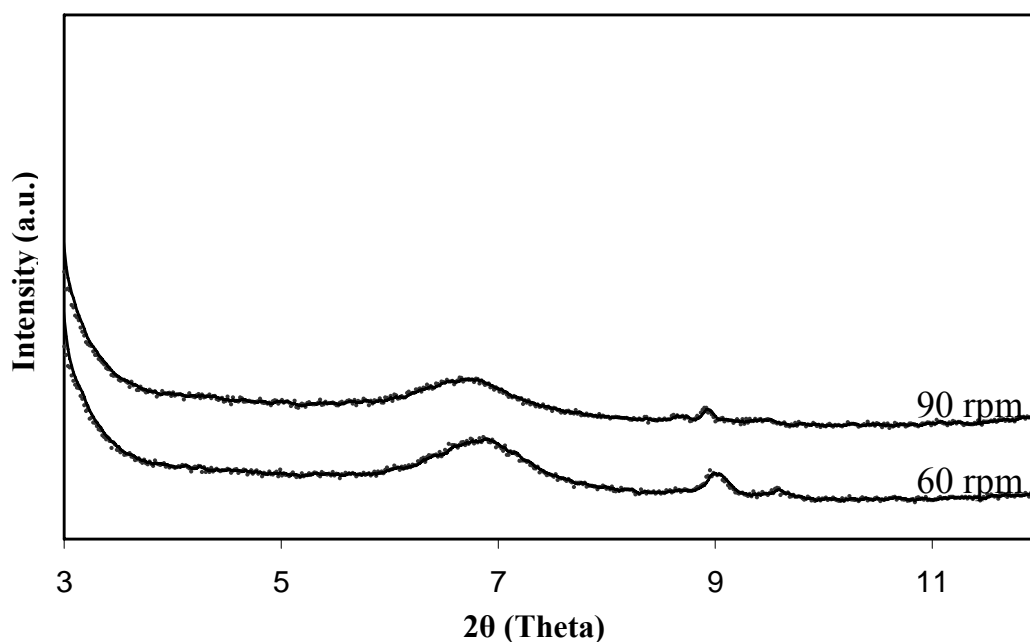


Figure 4. 8. XRD patterns of EPDM/ 10 wt. % OMMT nanocomposites with 60 and 90 rpm blending speed (blending time=15 min, blending temperature=150°C)

4.1.1. Examination of the Morphology of the Nanocomposites

In order to get a better insight into the clay dispersion with the nanocomposite, backscattered SEM images were taken from the fracture surface of neat EPDM and EPDM/OMMT nanocomposites. Fracture surfaces SEM image of neat EPDM after tensile testing was illustrated in Figure 4.9. The effects of blending time, temperature and speed on the fracture modes are shown in Figures 4.10 to 4.12 for 5 wt. % clay content and in Figures 4.13 to 4.15 for 10 wt. % clay content, respectively. Although some agglomeration of vulcanization chemicals and clay particles were observed on the surface of the EPDM/ 5 wt. % OMMT nanocomposites achieved by melt blending for 10 and 15 min, a complete dispersion of clay layers and other chemicals in the EPDM matrix was achieved when the blending time was set to 20 min.

In Figure 4.11, the effect of blending temperature on the morphology is illustrated. The EPDM/OMMT nanocomposites prepared by melt-blending at 120°C exhibit less agglomerate than those of the composites prepared at 150°C. This may be due to the thermal degradation of surfactant absorbed within the clay galleries by

temperature increase and friction within the compounder mills. The degradation of alkyl ammonium molecules may cause a lower degree of exfoliation than those for compounded nanocomposite structures at lower temperatures.

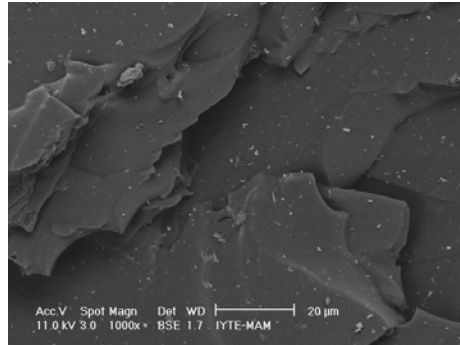


Figure 4. 9. Backscattered SEM fracture surface micrograph of neat EPDM after tensile testing

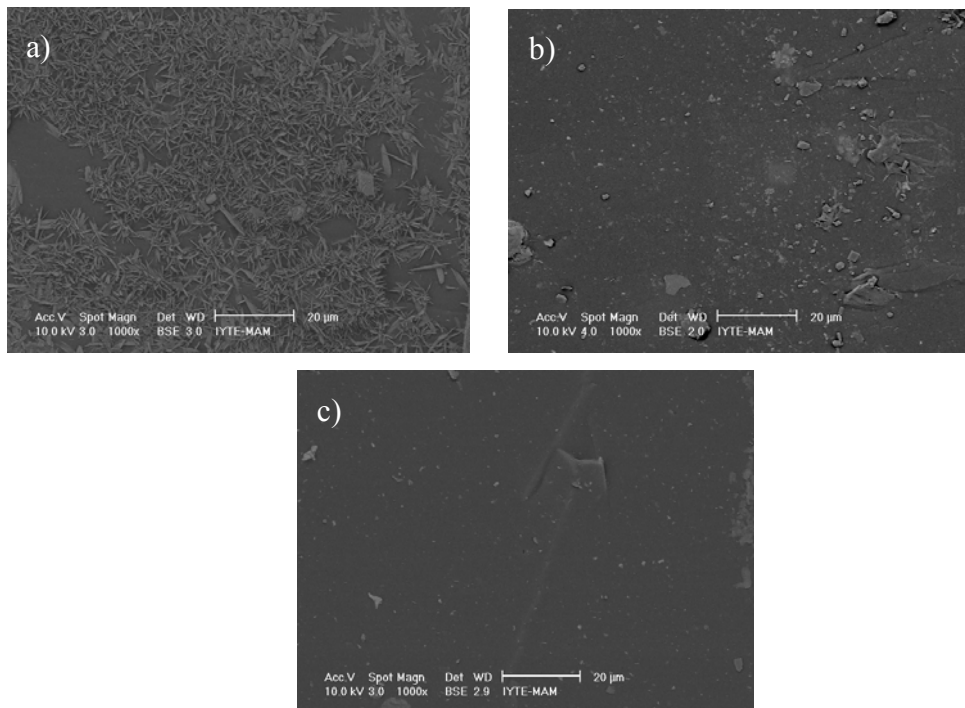


Figure 4. 10. Backscattered SEM fracture surface micrographs of EPDM/ 5 wt. % OMMT nanocomposite blended for a) 10, b) 15 and c) 20 min

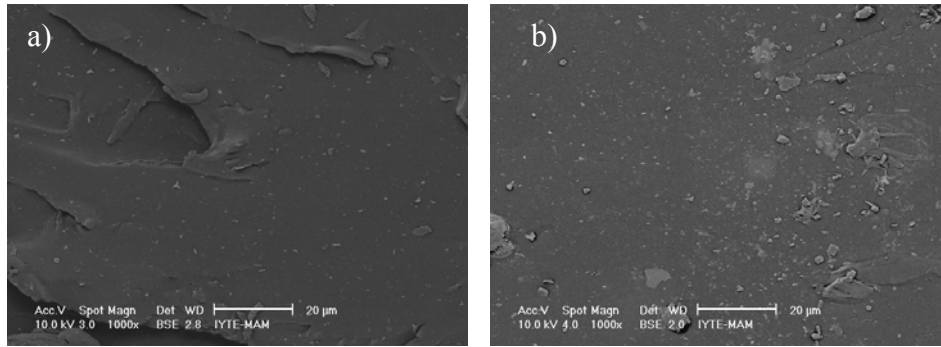


Figure 4. 11. Backscattered SEM fracture surface micrographs of EPDM/ 5 wt. % OMMT nanocomposite blended at a) 120 and b) 150°C

As shown in Figure 4.12, the blending speed for EPDM/5 wt. % OMMT systems has no obvious effect on the morphology by considering the amount of agglomeration on the fracture surfaces observed by SEM. It may be due to insufficient increase in the speed in the compounding process. Increasing the compounding speed from 60 to 90 did not really affect the microstructure of the nanocomposites produced, since the amount of shear was not high enough to obtain a homogenous OMMT distributed within the matrix in nanoscale.

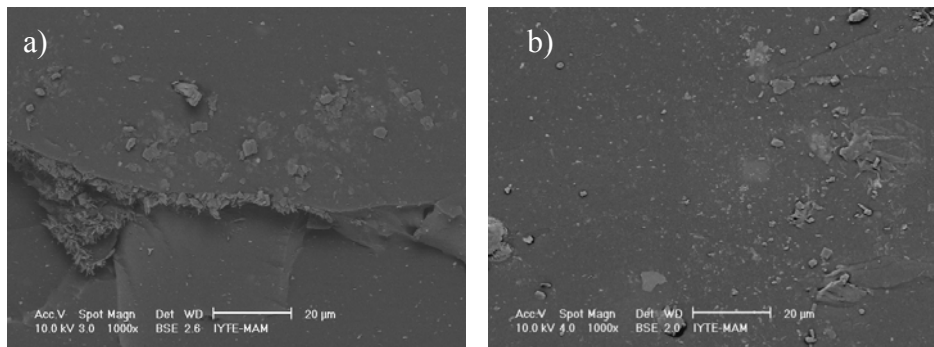


Figure 4. 12. Backscattered SEM fracture surface micrographs of EPDM/ 5 wt. % OMMT nanocomposite blended with a) 60 and b) 90 rpm

Figure 4.13 shows the SEM fracture surfaces for the nanocomposites prepared with various blending time. As the blending time increased, the shear effect imposed on the matrix increased, therefore the OMMT agglomerates were delaminated and better dispersed within the EPDM matrix. The same phenomenon described above is valid for 10 wt. % EPDM/OMMT nanocomposites. The degree of dispersion was not affected by the blending temperature and speed increases remarkably as seen in Fig.4.14 and 4.15, respectively. In addition, it was found that the fracture mechanism of the EPDM is altered by the addition of OMMT. The neat EPDM has a characteristic cross-hatched

failure pattern while OMMT/EPDM nanocomposites exhibit a typical line-flow pattern in their own fracture mechanisms. SEM images also revealed a homogenous dispersion of clay layers in the EPDM matrix. The degree of agglomeration decreases as the clay is modified with alkyl ammonium and EPDM matrix is compatibilized by EPDMgMA.

SEM elemental mapping technique was employed to determine the elemental distribution of the fracture surface of EPDM/OMMT nanocomposite as shown in Figure 4.16. The light-colored regions in the figures represent the elements denoted on each figure. It was seen that the agglomerations were emanated mostly by the zinc element. The results presented in Figure 4.16 support the XRD results stating the good dispersion of OMMT occurs within the EPDM matrix.

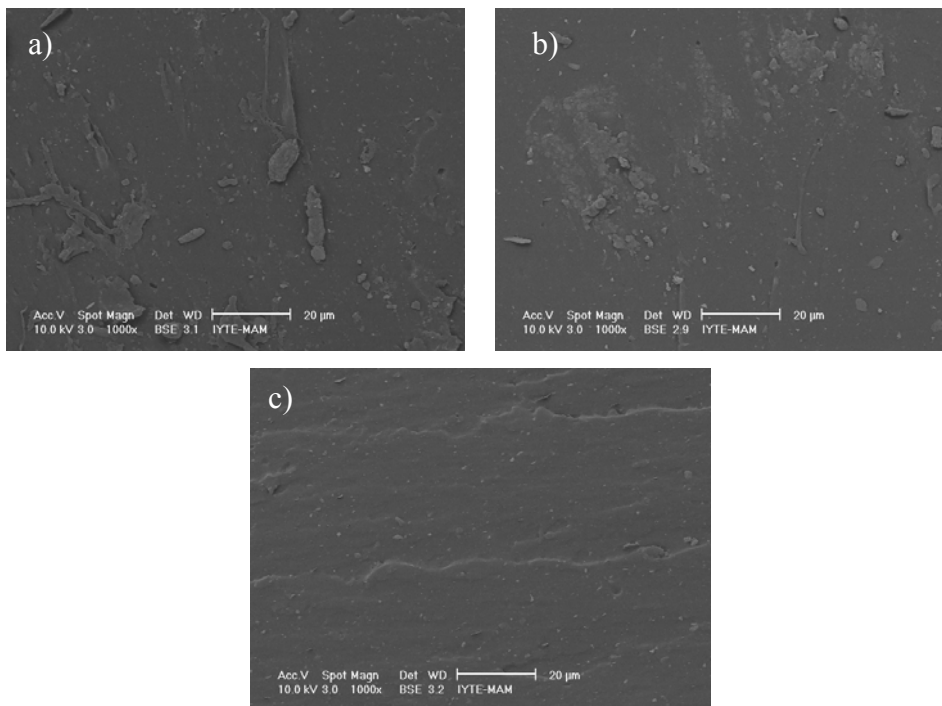


Figure 4. 13. Backscattered SEM fracture surface micrographs of EPDM/ 10 wt. % OMMT nanocomposite blended for a) 10, b) 15 and c) 20 min

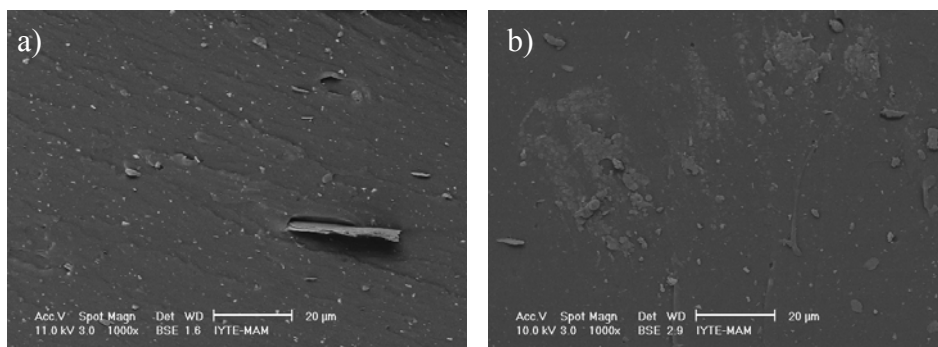


Figure 4. 14. Backscattered SEM fracture surface micrographs of EPDM/ 10 wt. % OMMT nanocomposite blended at a) 120 and b) 150°C

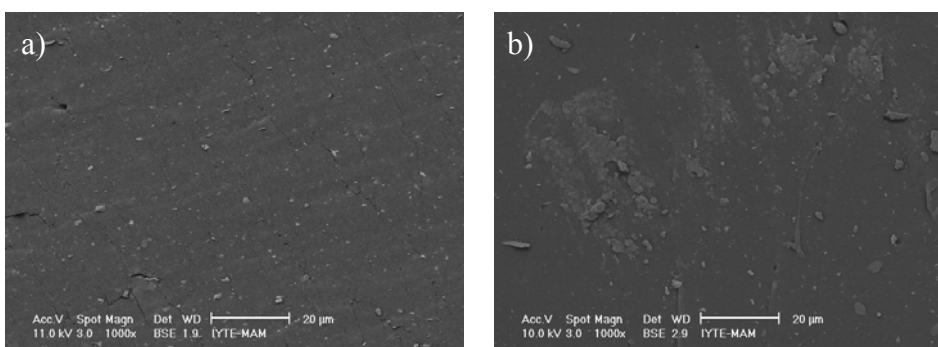


Figure 4. 15. Backscattered SEM fracture surface micrographs of EPDM/ 10 wt. % OMMT nanocomposite blended with a) 60 and b) 90 rpm

4.1.2. Fourier Transform Infrared Spectroscopy

The FTIR spectra of MMT, surfactant (octadecylamine) and organically modified MMT (OMMT) were recorded using KBr pellet method as shown in Figure 4.17.

The two characteristic bands at 3630 and 1032 cm^{-1} associates with the MMT-related groups, the stretching vibration of O–H bond and the stretching modes of the Si–O bond in the silicate groups, respectively. The peaks 1632 and 1424 cm^{-1} are due to C=C stretching of MMT. The peak at 520 cm^{-1} is due to Al–O stretching of MMT. The stretching vibrations of alkyl chain can be observed at 2920 and 2848 cm^{-1} and the bending vibrations of alkyl chain can be observed at 1472 cm^{-1} . The peak at 720 cm^{-1} is referred to the rocking vibrations of alkyl chain. The peaks in the characteristic band of octadecylamine at frequency of 2920 and 2848 cm^{-1} also appeared in the spectrum of organically modified MMT. This suggests that octadecylamine has tethered in between the silicate layers.

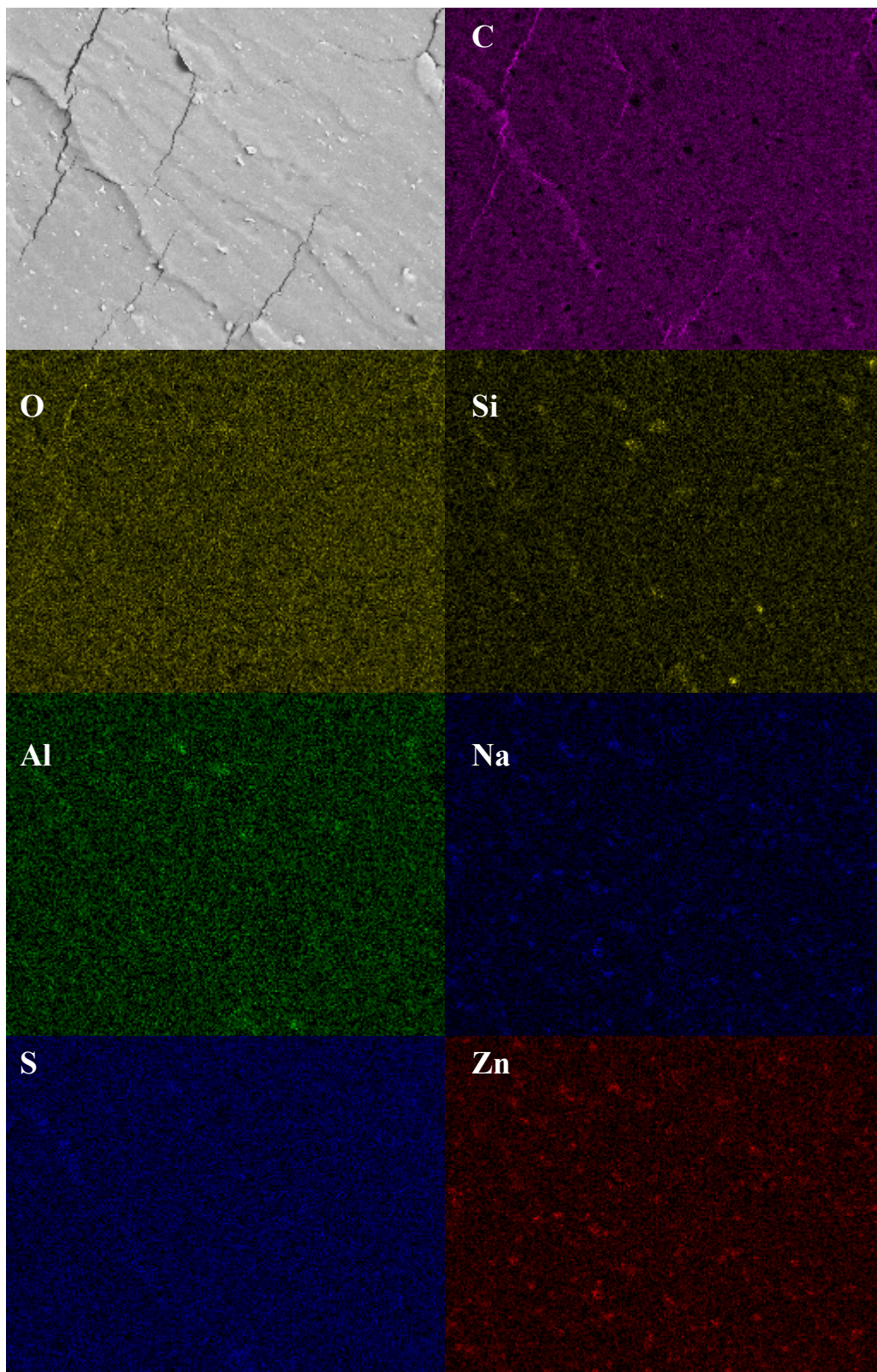


Figure 4. 16. SEM image and the corresponding maps of carbon, oxygen, silicon, aluminum, sodium, sulfur and zinc elements from the same surface

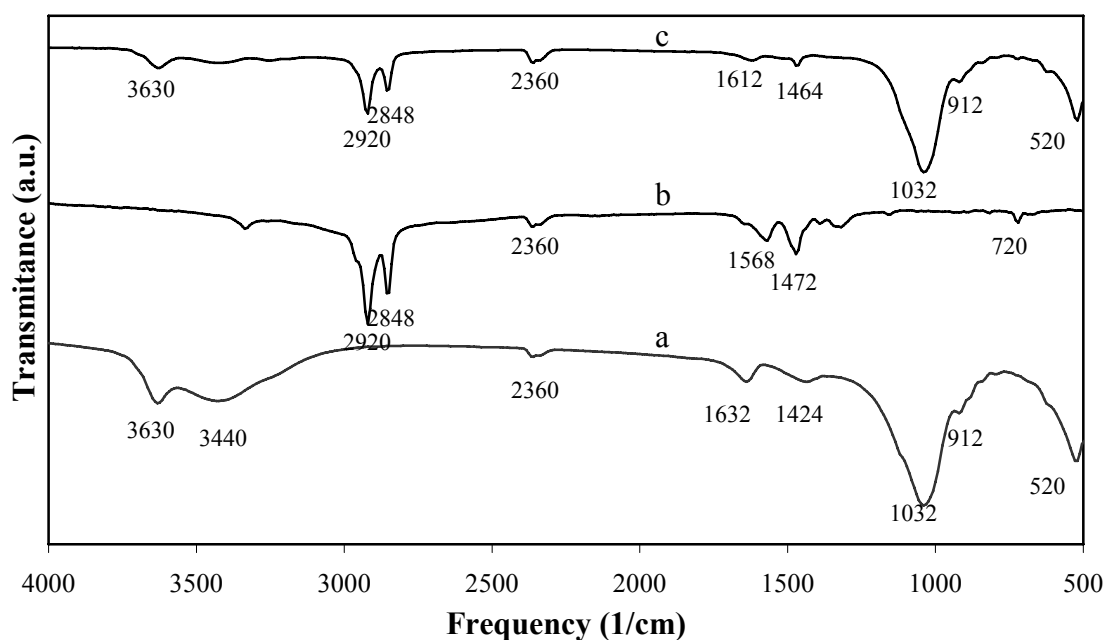


Figure 4. 17. FTIR spectra for (a) pure MMT, (b) surfactant (octadecylamine) and (c) organically modified MMT (OMMT)

4.2. Mechanical Properties of EPDM/Clay Nanocomposites

The effects of blending conditions (temperature of 120 and 150°C, blending speed of 60 and 90 rpm and blending time of 10, 15, 20 min), clay loading (5 wt. % and 10 wt. %) and aging conditions on the mechanical properties of EPDM/OMMT nanocomposites were investigated.

4.2.1. Tensile Properties of EPDM/Clay Nanocomposites and Effects of Aging Conditions

4.2.1.1. Effects of Blending Time on the Mechanical Properties

In the first stage, the mechanical properties of neat EPDM and EPDM/OMMT composites were examined by changing the blending time while the blending temperature and rotor speed were fixed at 150°C and 90 rpm, respectively. The neat

EPDM and its nanocomposites containing 5 and 10 wt. % OMMT were melt-blended for 10, 15 and 20 min. The tensile strengths of these samples before and after aging test are given in Figures 4.18 and 4.19, respectively. The average tensile strength of the neat EPDM was measured as 0.97 MPa. The tensile strength of the EPDM increased by 142.1%, and 315.8%, respectively with the addition of 5 and 10 wt. % of clays into the polymer matrix for blending time of 10 min.

When the results were compared obtained for different blending times, there was a dramatic decrease in the tensile strength of EPDM/ 10 wt. % OMMT nanocomposites when increasing blending time. On the other hand, the strength of neat EPDM and EPDM/ 5 wt. % OMMT nanocomposites remained almost constant. The plasticization effect of both alkyl ammonium surfactant and EPDMgMA compensates the tensile values as a decrement although the intercalation of EPDM molecules into the clay layers is promoted by longer blending time as seen in SEM characterization.

After aging test, the tendency of the results remained the same. As it can be seen from Figure 4.19 and Table 4.2, the loss in tensile strength after aging test increased with clay loading. The decrease on the tensile strength values of neat EPDM was found to be 13.86 %. When the same properties for EPDM/OMMT nanocomposites were evaluated, the decrease in tensile strength was 35.65 % for nanocomposite with 5 wt. % of OMMT and 36.71 % for those prepared with 10 wt. % OMMT. However, the lowest tensile strength values of 5 and 10 wt. % OMMT containing EPDM nanocomposites after aging test was found to be still higher than those of neat EPDM. It was also seen that the decrease of tensile strength after aging test increased with blending time. These results imply that the incorporation of OMMT into EPDM matrix improves the degradation behavior of the nanocomposites. This is due to the barrier effect of the dispersed clay layers on the diffusion path of water within the EPDM matrix. As the OMMT content increases, the barrier effect of the clay layers become more significant. Thus, the decrease in strength values is lower in nanocomposites with higher OMMT content.

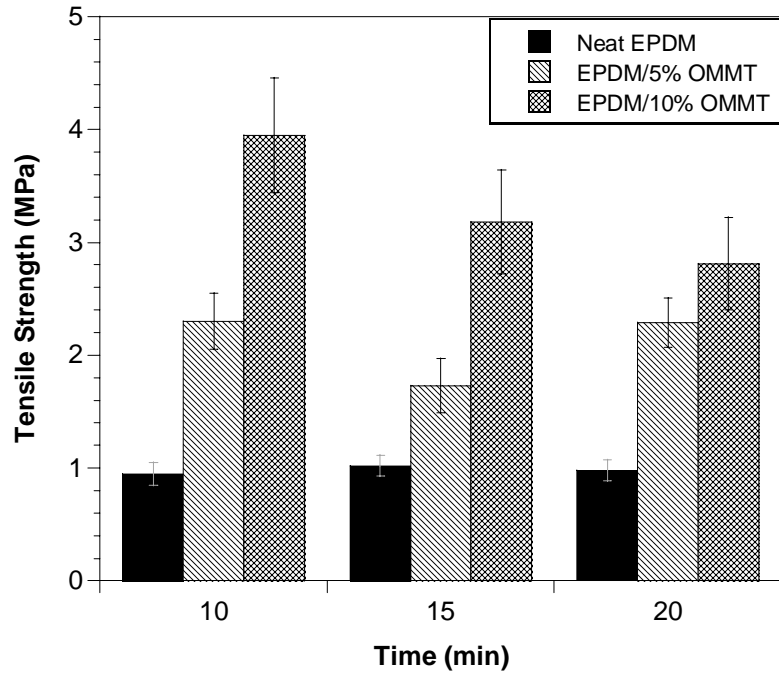


Figure 4. 18. Prior to aging, tensile strength values of neat EPDM and its nanocomposites containing 5 and 10 wt. % of OMMT with respect to various blending times including 10, 15 and 20 min.

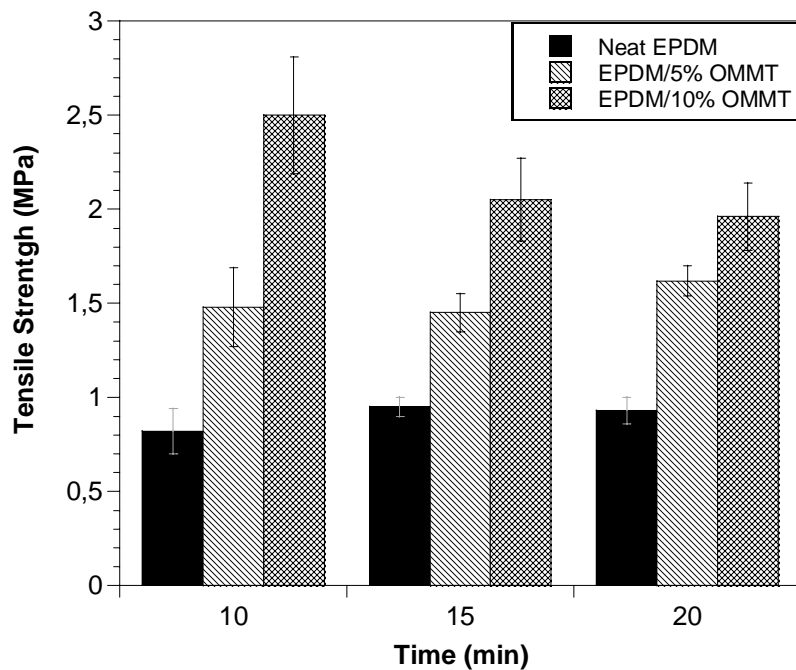


Figure 4. 19. After aging process tensile strength values of neat EPDM and its nanocomposites containing 5 and 10 wt. % of OMMT with respect to various blending times including 10, 15 and 20 min.

Table 4. 1. Loss in tensile strength after aging test

Time	Neat EPDM	EPDM/5 wt. % OMMT	EPDM/10 wt. % OMMT
10	13.68 %	35.65 %	36.71 %
15	6.86 %	16.19 %	35.54 %
20	5.01 %	29.26 %	30.25 %

The same behavior seen in strength values was observed when the other mechanical properties of the nanocomposites, such as elongation at break and modulus at 100% elongation are evaluated as seen in Table 4.2. The increase in OMMT within the nanocomposite structure by mass, improves these mechanical properties. However, it was obtained that as the amount of modified clay increased in polymer matrix, the mechanical properties were not always affected positively. The increase in the amount of modified clay increases the amount of surfactant and the compatibilizer which causes a plasticization effect within the structure. On the other hand, as the blending time was increased, the temperature of the nanocomposite system was increased because of the shear stress as a result of friction. That phenomenon also causes the degradation of polymeric molecules indicating a loss in mechanical strength.

Table 4. 2. Effect of aging, mixing time and the OMMT content on elongation at break, modulus at 100% extension and tear strength for neat EPDM and EPDM/OMMT nanocomposites (Standard deviations are given in parenthesis)

Blending Time	10 min			15 min			20 min			
	Neat EPDM	EPDM / 5%OMMT	EPDM / 10%OMMT	Neat EPDM	EPDM / 5%OMMT	EPDM / 10%OMMT	Neat EPDM	EPDM / 5%OMMT	EPDM / 10%OMMT	
Elongation at Break (%)	Before aging	163.87 (±33.37)	240.20 (±20.60)	357.86 (±27.38)	179.80 (±21.27)	182.69 (±17.06)	333.62 (± 34.53)	164.61 (±23.31)	252.43 (±26.23)	284.76 (±29.62)
	After aging	124.33 (±19.97)	189.83 (±36.59)	328.66 (±37.79)	156.57 (±16.89)	172.19 (±15.29)	275.37 (±28.23)	164.88 (±16.47)	228.80 (±23.13)	257.44 (±32.18)
Modulus at %100 Elongation (MPa)	Before aging	0.74 (±0.01)	1.13 (±0.02)	1.31 (±0.06)	0.74 (±0.01)	1.11 (± 0.01)	1.23 (± 0.04)	0.72 (±0.02)	1.12 (±0.04)	1.24 (±0.02)
	After aging	0.74 (±0.01)	1.03 (±0.07)	1.15 (±0.04)	0.75 (±0.01)	1.08 (±0.02)	1.12 (±0.02)	0.75 (±0.05)	0.98 (±0.07)	1.13 (±0.02)

4.2.1.2. Effects of Blending Temperature on the Mechanical Properties

To investigate the effects of blending temperature on the mechanical properties of neat EPDM and its nanocomposites containing 5 and 10 wt. % OMMT, the blending temperature and OMMT content were altered; while the blending speed and time were fixed at 90 rpm and 15 min. Figure 4.20 shows the tensile strengths of neat EPDM and EPDM/OMMT nanocomposites which were blended at 120 and 150°C. The tensile strength of neat EPDM was measured as 0.85 and 0.93 MPa for 120° and 150°C, respectively. It was observed that addition of OMMT into EPDM matrix significantly improves the tensile strength of the polymer matrix. As an example, at blending temperature of 120°C, addition of 5 and 10 wt. % of OMMT increases the average tensile strength of neat EPDM by 148 % and 281 %, respectively. On the other hand, as the blending temperature is increased from 120° to 150°C, the tensile strength of neat EPDM and EPDM/OMMT nanocomposites remained almost constant.

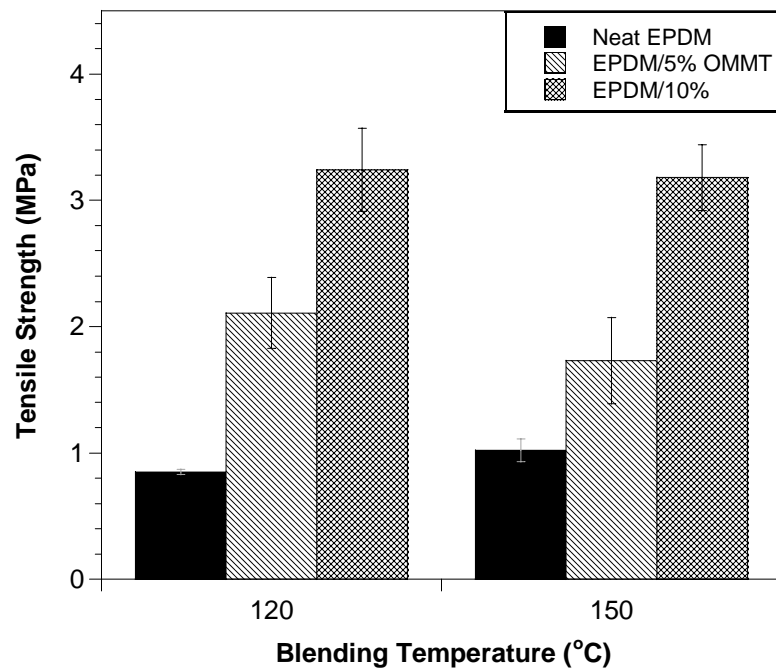


Figure 4. 20. Prior to aging, tensile strength values of neat EPDM and its nanocomposites containing 5 and 10 wt. % of OMMT with respect to blending temperatures of 120 and 150°C

In Figure 4.21, the tensile strength values of the neat EPDM and its nanocomposites after aging test are shown and in Table 4.3 the percentages of loss in tensile strength values

are given for these samples after aging test. It was observed that although the reduction in the tensile strength of neat EPDM increased by increasing the blending temperature, the percentage of the loss in strength values remained almost the same for the nanocomposites.

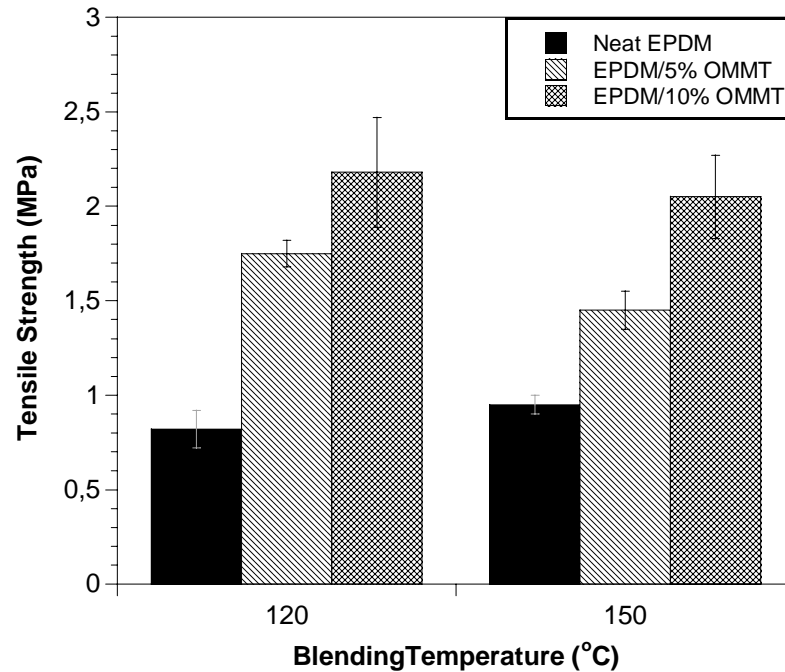


Figure 4. 21. After aging, tensile strength values of neat EPDM and its nanocomposites containing 5 and 10 wt. % of OMMT with respect to blending temperatures of 120 and 150°C

Table 4. 3. Loss in tensile strength after aging test

Blending Temperature (°C)	Neat EPDM	EPDM/5 wt. % OMMT	EPDM/10 wt. % OMMT
120	3.53%	17.06%	32.72%
150	6.86%	16.18%	35.53%

Table 4.4 exhibits the tensile elongation at break and modulus values of neat EPDM and its nanocomposites before and after aging test. The neat EPDM exhibited an elongation at break values of 135.16 % and 0.74 MPa, respectively. Similar to tensile strength values, addition of OMMT into EPDM matrix significantly improves the elongation at break and modulus values. For 120°C blending temperature, the average elongation at break and modulus values of neat EPDM is improved by 76.4 %, and 52.7 % for 5 wt. % OMMT addition and by 133.5 % and 77 % for 10 wt. % OMMT addition. The elongation at break

values increases due to increased temperature from 120°C to 150°C for neat EPDM. However, for EPDM/5% OMMT nanocomposites, as the temperature of blending increased from 120 °C to 150 °C, elongations at break values were dropped by 18 % and 23.36 %, respectively. For EPDM/10 wt.% OMMT system, the increase of blending temperature resulted with the increase of elongation at break value, while the other mechanical properties remained almost constant. These results imply that clay layers within EPDM matrix has a strong reinforcement effect that the strength and stiffness values are significantly improved by the presence of clay layers. In addition to improvements on the strength values, the significant improvements on the elongation values imply that the toughness of the EPDM is increased by the incorporation of clay layers with the EPDM matrix.

4.2.1.3. Effects of Blending Speed on the Mechanical Properties

To investigate the effect of blending rotor speed on the properties, blending temperature and time were fixed at 150°C and 15 min, respectively. The mechanical properties of neat EPDM and its nanocomposites containing 5 and 10 wt. % OMMT which were blended with 60 and 90 rpm were compared. Figure 4.22 shows the tensile strength of the neat EPDM and EPDM/OMMT nanocomposites by changing the blending rotor speed from 60 to 90 rpm. Increasing the rotor speed increased the tensile strength of neat EPDM and EPDM/10 wt. % OMMT nanocomposites while the tensile strength of EPDM/5 wt. % OMMT nanocomposite decreased. Figure 4.23 shows the tensile strength values of neat EPDM and its nanocomposites after aging test. When the results were compared with the values before aging, it inferred that higher rotor speeds enhanced the loss in tensile strength values with aging.

Table 4.6 compares the elongation at break and tensile modulus values of the neat EPDM and its nanocomposites before and after the aging test. Similar to tensile strength values, addition of OMMT into EPDM matrix significantly improves the elongation at break and modulus values. For 60 rpm blending rotor speed, the average elongation at break and tensile modulus values of neat EPDM (149.17 %, and 0.74 MPa) is improved by 59 %, and 54 % for 5 wt. % OMMT addition and by 76.77 %, and 70.27 % for 10 wt. % OMMT addition. The tensile strength, elongation at break and tensile modulus values increases due to increased rotor speed from 60 rpm to 90 rpm for neat EPDM and EPDM/10% OMMT nanocomposite while tensile modulus values remain almost constant for the same case.

Table 4. 4. Effect of temperature on elongation at break and modulus at 100% extension for neat EPDM and EPDM/OMMT nanocomposites
(Standard deviations are given in parenthesis)

Blending Temperature (°C)		120			150		
		Neat EPDM	EPDM / 5%OMMT	EPDM / 10%OMMT	Neat EPDM	EPDM / 5%OMMT	EPDM / 10%OMMT
Elongation at Break (%)	Before aging	135.16 (± 7.44)	238.36 (± 27.06)	315.63 (± 27.54)	179.80 (± 21.27)	182.69 (± 17.06)	333.62 (± 34.53)
	After aging	126.91 (±24.75)	217.72 (±9.72)	280.12 (±37.15)	156.57 (±16.89)	172.19 (±15.29)	275.37 (±28.23)
Modulus at %100 Elongation (MPa)	Before aging	0.74 (± 0.02)	1.13 (± 0.03)	1.31 (± 0.03)	0.74 (± 0.01)	1.11 (± 0.01)	1.23 (± 0.03)
	After aging	0.75 (±0.01)	1.08 (±0.01)	1.15 (±0.05)	0.75 (±0.01)	1.08 (±0.02)	1.12 (±0.02)

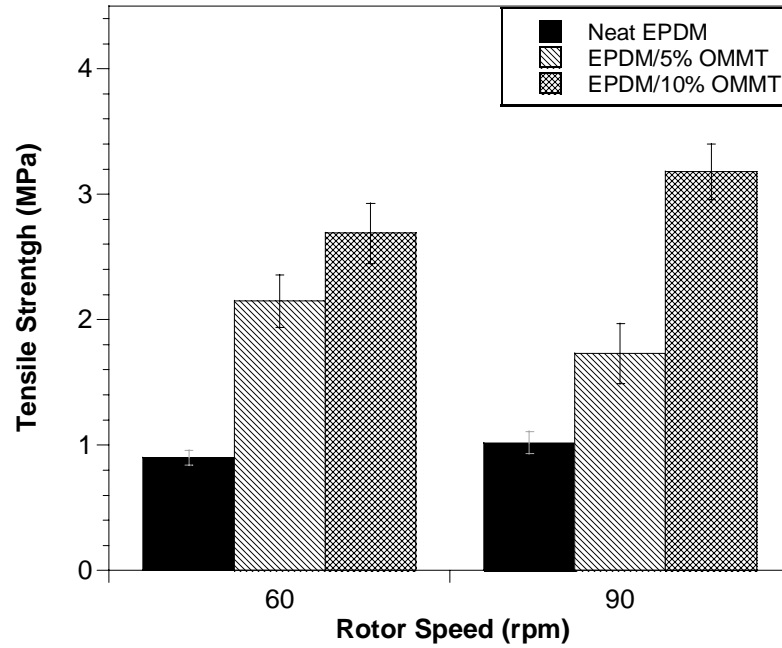


Figure 4. 22. Prior to aging, tensile strength values of neat EPDM and its nanocomposites containing 5 and 10 wt. % of OMMT with respect to blending speeds of 60 and 90 rpm

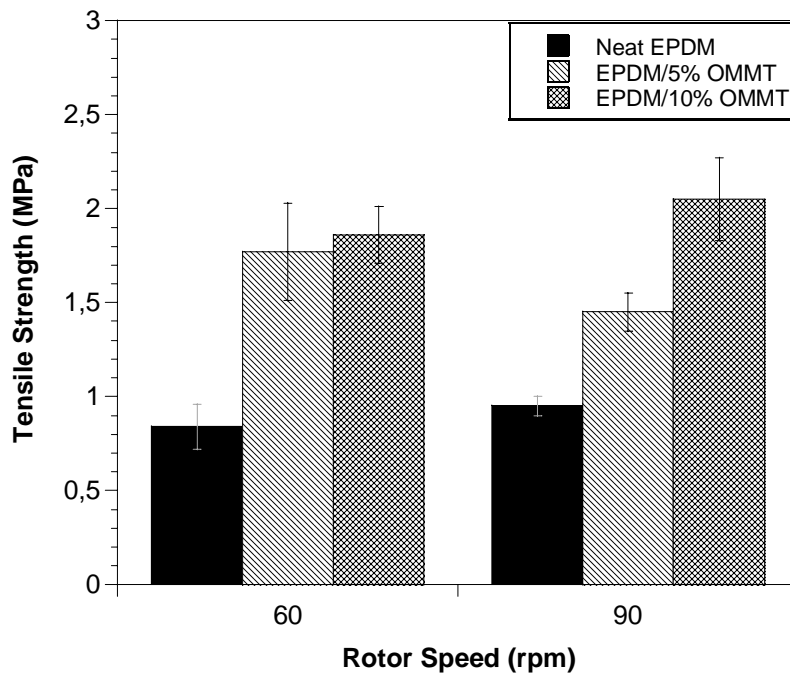


Figure 4. 23. After aging, tensile strength values of neat EPDM and its nanocomposites containing 5 and 10 wt. % of OMMT with respect to blending speeds of 60 and 90 rpm

Table 4. 5. Loss in tensile strength after aging test

Speed (rpm)	Neat EPDM	EPDM/5 wt. % OMMT	EPDM/10 wt. % OMMT
60	7.14%	17.67%	30.85%
90	7.37%	16.18%	35.53%

For EPDM/5 wt. % OMMT nanocomposite, as the blending rotor speed increased from 60 rpm to 90 rpm, the tensile strength, elongation at break, and tensile modulus at 100% elongation values were dropped by 19.53 %, 23 %, 2.6 %, 12.2 %, respectively. These results imply that the shear forces applied on the silicate layers increases due to blending rotor speed. The increased forces improve the intercalation of the silicate layers and results with better dispersion of the silicate layers within the EPDM matrix.

4.2.2. Hardness of Nanocomposites and Influence of Aging Test on Hardness

The hardness values of neat EPDM and EPDM/OMMT nanocomposites before and after aging are compared in Figure 4.24. The average hardness values for neat and EPDM based nanocomposites with 5 and 10 wt. % OMMT was measured as 40, 49, and 52 Shore A, before aging. It was found that the hardness of the composites was only slightly affected by the aging. After aging, the values were decreased by about 5, 2 and 2% for neat EPDM and EPDM/OMMT nanocomposites with 5 and 10 wt. % OMMT, respectively.

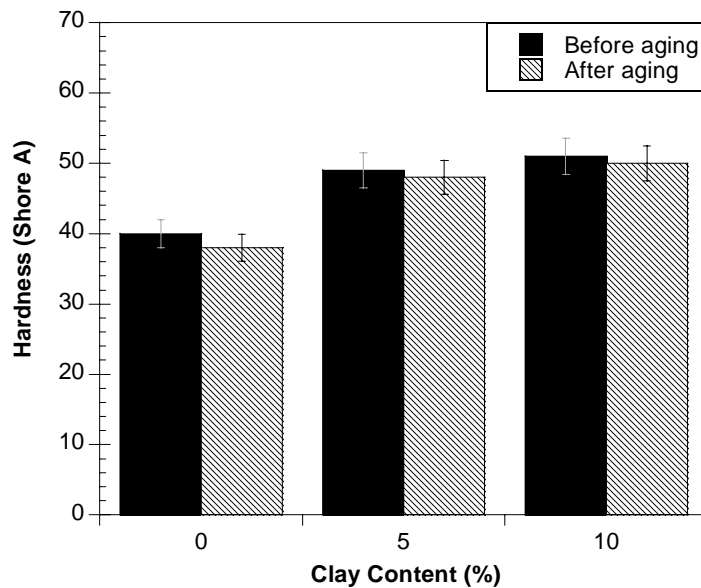


Figure 4. 24. Effect of clay addition and aging on hardness values of EPDM and its nanocomposites

Table 4. 6. Effect of aging, rotor speed and the OMMT content on elongation at break and modulus at 100% extension for neat EPDM and EPDM/OMMT nanocomposites (Standard deviations are given in parenthesis)

Blending Rotor Speed (rpm)		60			90		
		Neat EPDM	EPDM / 5%OMMT	EPDM / 10%OMMT	Neat EPDM	EPDM / 5%OMMT	EPDM / 10%OMMT
Elongation at Break (%)	Before aging	149.17 (± 15.24)	237.19 (± 22.37)	263.69 (± 20.33)	179.80 (± 21.27)	182.69 (± 17.06)	333.62 (± 34.53)
	After Aging	149.43 (±17.67)	218.7 (±22.37)	250.73 (±28.39)	156.57 (±16.89)	172.19 (±15.29)	275.37 (±28.23)
Modulus at %100 Elongation (MPa)	Before aging	0.74 (± 0.01)	1.14 (± 0.02)	1.26 (± 0.02)	0.74 (± 0.01)	1.11 (± 0.01)	1.23 (± 0.04)
	After Aging	0.70 (± 0.01)	1.08 (± 0.03)	1.11 (± 0.03)	0.75 (± 0.01)	1.08 (± 0.02)	1.12 (± 0.02)

4.2.3. Tear Properties of EPDM/Layered Clay Nanocomposites

To evaluate the mechanical properties of the nanocomposites developed in this study, tear test was also performed. The tear strength of OMMT/EPDM nanocomposites was investigated to determine the effects of clay concentration, blending time, temperature and speed on the tear properties.

As shown in Figure 4.25, the tear strength of the neat EPDM was measured as 4.32 kN/M for blending time of 10 min. Addition of modified clay layers (OMMT) increased the tear strength values of neat EPDM. As the tear strength of 5 wt. % OMMT/EPDM nanocomposite increased slightly with time, 10 wt. % OMMT/EPDM nanocomposites showed the same behavior with neat EPDM. At high clay contents, the amount of surfactant and compatibilizer were increased resulting in plasticization effect negatively the tear strength.

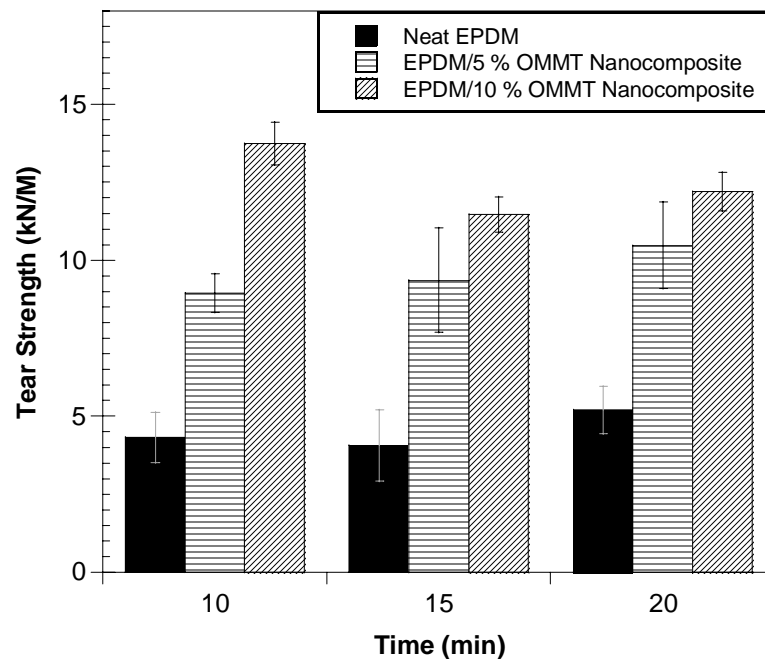


Figure 4. 25. Tear strength values for neat EPDM and its nanocomposites containing 5 and 10 wt. % OMMT blended for 10, 15 and 20 min

When the influence of the blending temperature and blending speed were investigated, there was not any significant affect of the blending temperature and speed on the tear strength of neat EPDM and OMMT/EPDM nanocomposites as shown in Figures 4.26 and 4.27, respectively. The tear strength values showed a very similar tendency with other tensile properties.

By 5 wt. % addition of clay, while the tear strength of neat EPDM was increased about 158.7% at blending temperature of 120°C, it was increased about 130.5% at blending temperature of 150°C. On the other hand, when the rotor speed was 60 rpm, the addition of 5 wt. % clay increased the tear strength of neat EPDM about by 176.9%. Moreover, addition of 10 wt. % OMMT increased this value by 182.9%.

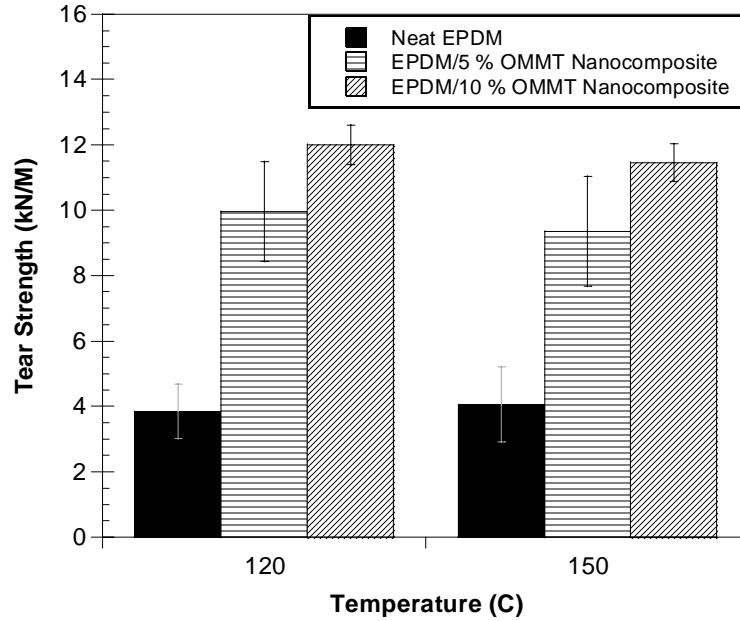


Figure 4. 26. Tear strength values for neat EPDM and its nanocomposites containing 5 and 10 wt. % OMMT and blended of 120 and 150 min

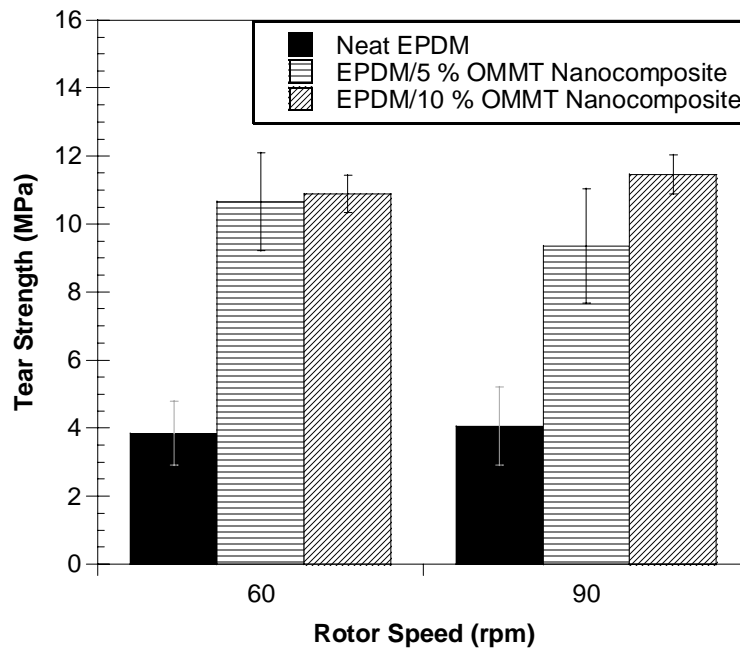


Figure 4. 27. Tear strength values for neat EPDM and its nanocomposites containing 5 and 10 wt. % OMMT blended with rotor speed of 60 and 90 rpm

4.3. Thermal Properties of Nanocomposites

4.3.1. Thermogravimetric Analysis (TGA)

Figure 4.28 shows typical thermogravimetric analysis (TGA) weight loss curves of neat EPDM and its nanocomposites containing 5 and 10 wt. % OMMT. The TGA curves exhibited two stages. There is a small weight loss up to 200°C indicating the thermal stability of the material up to this temperature. “Highly volatile matter” may contain a low boiling fraction consisting of moisture, polymer diluents, curatives (sulfur, accelerator and antioxidants) in this temperature range. Between 200-400°C, an initial weight loss occurs due to the loss of volatile matter present in the composition. The maximum temperature (T_{max}) corresponding to the described weight loss occurs at around 310°C. This is generated by oil volatilization without any polymer degradation. To determine the oil content in EPDM, the TG curve is overlaid which means a complete oil loss. The TGA curve is overlaid until the oil loss is complete. As seen in Figure 4.28, the weight loss reaches to 60 wt. % after the oil removal from the polymeric system. Based on this information, it was revealed that the oil content is nearly 40 wt. % in EPDM/OMMT nanocomposites which is consistent with the data that is given in the Chapter 3. On TGA graphs, further weight loss occurs in the 450-490°C range, due to the medium volatile elastomeric components present in the composition. Furthermore, the weight value does not reach to zero point because of the ash, zinc oxide and fillers or reinforcing materials in EPDM composite. The fraction of the residue increases with the increase of organoclay content with the polymer matrix, as presented in Figure 4.28.

Ahmadi , et al. (Ahmadi , et al. 2005) also reported the increase in thermal stability of EPDM/clay hybrids with clay loading. Earlier studies reported that composites with good dispersion of organoclay exhibits higher stability (Mousa A. 2006). This result agrees with the significant feature of nanoscale particulate nanocomposites in which improved thermal stability can be reached at very low loadings of the nanofillers. The thermal behavior of EPDM/clay nanocomposites were also studied by Acharya et.al. and they observed that the coexistence of intercalated and exfoliated silicate layers in the EPDM matrix restrict the thermal motion of EPDM polymer segments by the improvement of Si-O-C interfacial interaction. The decomposition temperatures of samples were determined by derivatives of TGA curves

as shown in Figure 4.29 that indicates the decomposition temperature of the composites. The decomposition temperatures of the samples that were prepared in this study are listed in Table 4.7. It can be concluded that the EPDM/layered silicate nanocomposites exhibits slightly higher thermal stability as compared to neat EPDM. This improvement is attributed to the nanoscale clay platelets within the EPDM network that delays diffusion of the volatile decomposition compounds out from the nanocomposite structure.

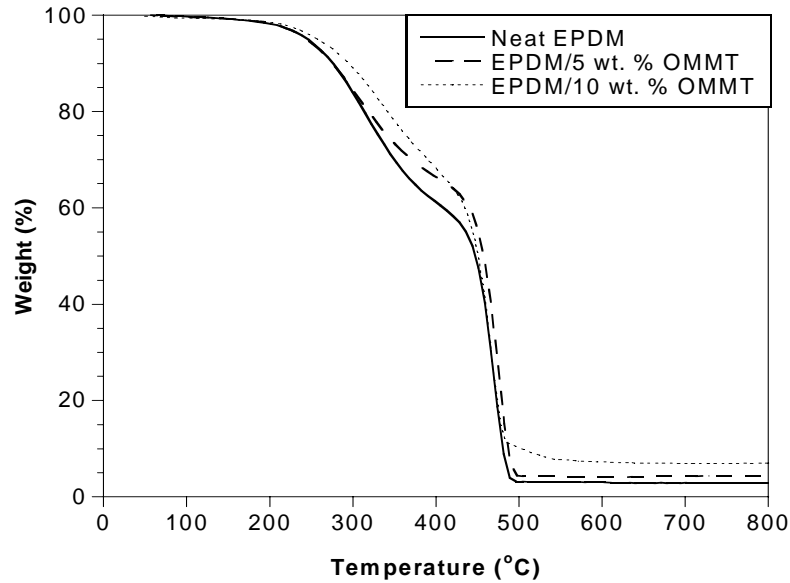


Figure 4. 28. The effect of organoclay (OMMT) content on the TGA thermograms of EPDM

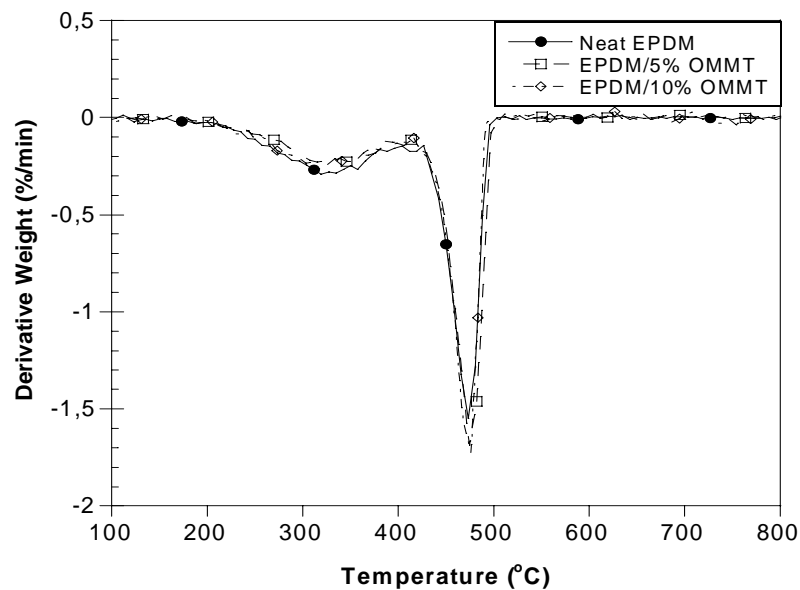


Figure 4. 29. Typical TGA thermogram and its derivative curves of neat EPDM and EPDM/OMMT nanocomposites

Table 4. 7. Decomposition temperatures of neat EPDM and OMMT nanocomposites prepared with various content and processing conditions

		Neat EPDM	EPDM/5 wt. % OMMT	EPDM/10 wt. % OMMT
Time (min)	10	469.69	474.40	469.78
	15	471.10	471.27	475.36
	20	469.87	476.65	475.76
Temperature (°C)	120	475.32	475.55	475.07
	150	471.10	471.27	475.36
Speed (rpm)	60	472.79	482.12	476.82
	90	471.10	471.27	475.36

4.3.2. Differential Scanning Calorimetry (DSC)

Figure 4.30 shows DSC thermograms of neat EPDM and EPDM/OMMT nanocomposites. The glass transition temperature (T_g) values of nanocomposites insignificant decrease with clay loading. Such a behavior was also observed by Acharya , et al. for EPDM/modified clay systems and was attributed to the reduction in cohesive forces of attraction between polymer chains. The reduction in cohesive forces between the polymer chains increased the mobility leading to a decrease in T_g . On the other hand, the decrease in T_g that was caused by the addition of the clay in EPDM was related to the amount of surfactant used for clay modification.

As seen from Table 4.8, the T_g values were not affected by the process conditions significantly. The minor reduction of T_g values due to assition of OMMT into EPDM may be related with the plastisizing effect of the surfactant used for surface modification of the clay layers. There was not much study about the thermal characterization of the EPDM/organoclay nanocomposite systems by DSC.

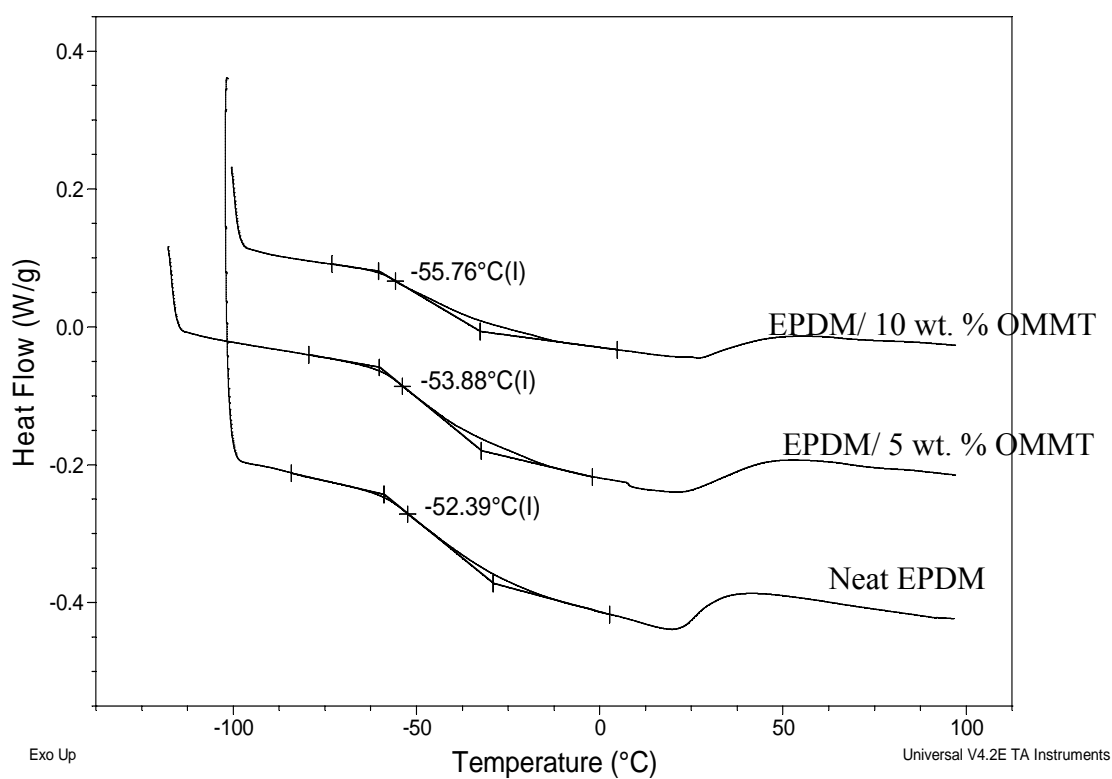


Figure 4. 30. DSC thermograms for neat EPDM and its nanocomposites containing 5 and 10 wt. % OMMT

Table 4. 8. Glass transition temperatures (T_g) of EPDM and its nanocomposites processed under various conditions

		Neat EPDM	EPDM/5 wt. % OMMT	EPDM/10 wt. % OMMT
Time (min)	10	-51.72	-53.89	-53.11
	15	-52.39	-53.88	-55.76
	20	-54.73	-53.31	-53.70
Temperature (°C)	120	-50.46	-51.42	-52.96
	150	-52.39	-53.88	-55.76
Speed (rpm)	60	-51.68	-52.70	-53.94
	90	-52.39	-53.88	-55.76

4.3.3. Dynamic Mechanical Analysis (DMA)

To investigate the effect of layered clays on the thermo-mechanical properties of the EPDM, the dynamic mechanical analysis (DMA) was performed. Figure 4.31 (a) shows that the EPDM/ OMMT nanocomposites exhibit slightly higher storage modulus values than neat EPDM due to the reinforcing effect of OMMT layers distributed in the polymer matrix. As an example, the storage modulus at 25°C of EPDM nanocomposites containing 5 wt. % OMMT is 2.1 times higher than that of neat EPDM. Similarly, Liu , et al. found that the storage modulus at 25 °C of EPDM with 7.5 wt. % organoclay loading is 3.9 times higher than that of neat EPDM. The similar observations were also found by Ahmadi , et al. and Gatos , et al. that is ascribed to maximum adhesion between the polymer matrix and the layers surfaces, because of nanometer size. The nanolayers restrict the mobility of the EPDM molecular chains.

On the other hand, no effects of process conditions were observed on the thermo-mechanical behavior of the composites. Figure 4.31 (b) shows $\tan \delta$ versus temperature values for neat EPDM and its nanocomposites. As seen in the figure, the addition of OMMT generates a minor shift in T_g which is determined from the peak of the $\tan \delta$ curve, toward a higher temperature. It was also seen that, there is a reduction in $\tan \delta_{\max}$ values with addition of OMMT. This observation confirms the previous findings.

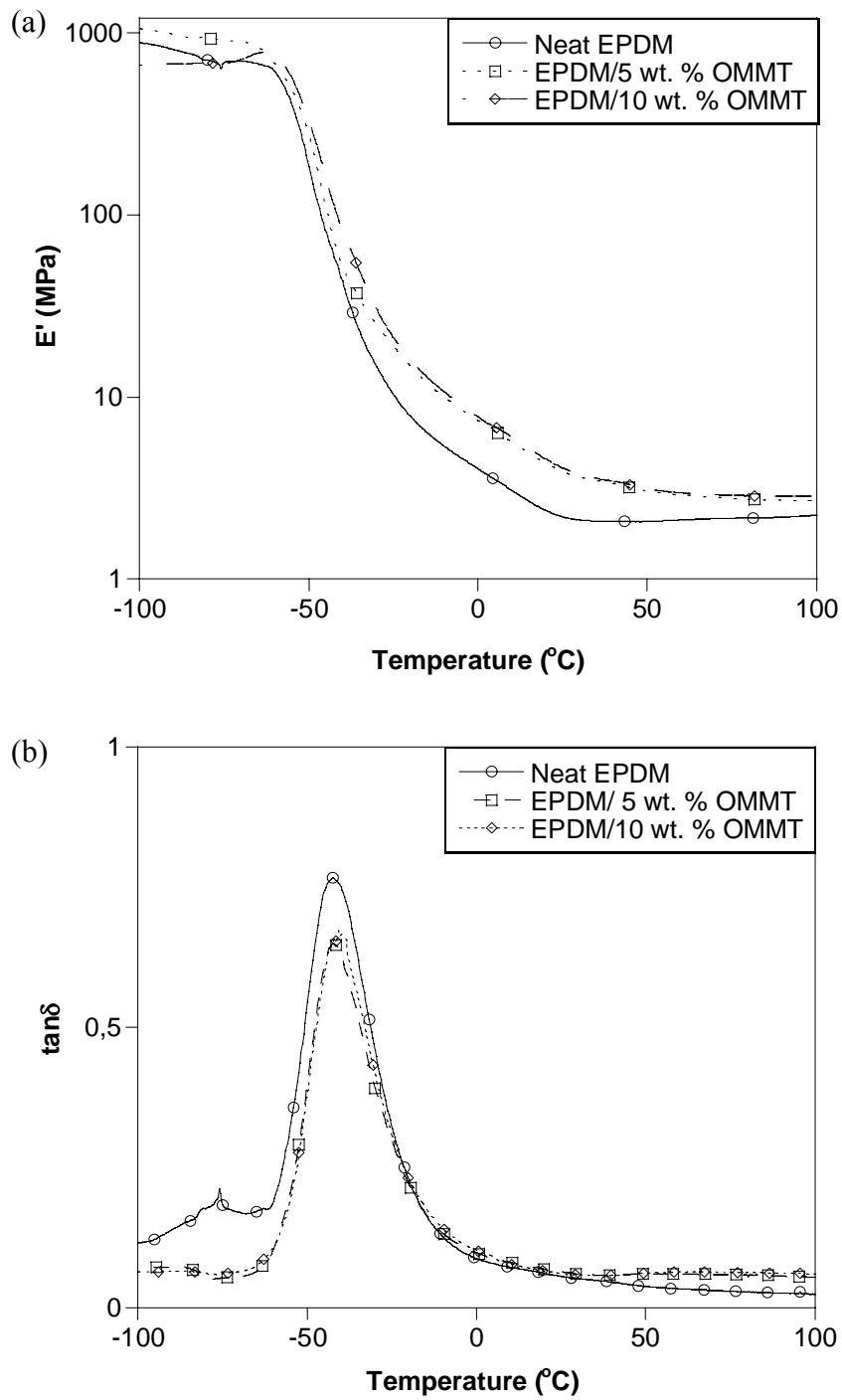


Figure 4. 31. Dynamic mechanical analysis (DMA) spectra: a) Storage modulus (E') and b) $\tan \delta$ as a function of temperature for the neat EPDM and its nanocomposites containing 5 and 10 wt. % OMMT

CHAPTER 5

CONCLUSION

This work revealed the effects of clay content, mixing conditions, chemical aging on the mechanical behavior of ethylene-propylene-diene-rubber (EPDM)/organo modified clay (OMMT) nanocomposites. EPDM/OMMT nanocomposites were successfully prepared by melt-blending octadecylamine modified montmorillonite and EPDMgMA as a compatibilizer with EPDM matrix. Silicate particles were treated with octadecylamine through an ion exchange reaction. In this way, Na^+ interlayer cations of the silicate is exchanged with onium cation of the surfactant that turns the hydrophilic silicates to organophilic characteristics.

Microstructure-property relation within the developed nanosystems was investigated at a fundamental level based on (XRD), scanning electron microscopy (SEM) techniques. Tensile strength, elongation at break and modulus at 100% elongation values; seperately tear strength of the nanocomposites was measured using mechanical and tear testing. Thermal behavior was monitored with thermogravimetric analysis (TGA), differential scanning calorimeter (DSC) and dynamic mechanical analysis (DMA). And also to investigate the effect of aging environment on the mechanical properties of the neat EPDM and EPDM/OMMT nanocomposites, mechanical tests were performed.

XRD patterns showed that the basal spacing of modified montmorillonite increases from 14.6 to 30.9Å promoting the penetration of polymeric molecules into the clay galleries for exfoliation. XRD patterns of the EPDM nanocomposites containing OMMT shows that the characteristic peaks of the silicates are not detectable for the nanocomposites samples at process conditions of 150°C, 20 min, 60 rpm. This indicates the further intercalation of the silicates within the polymer matrix.

Based on SEM, it was observed that as the blending time increased, the shear effect imposed on the matrix increased; therefore the OMMT agglomerates were delaminated and better dispersed within the EPDM matrix. It was also found that the fracture mechanism of the EPDM is altered by the addition of OMMT. In addition, it was found that the neat EPDM has a characteristic cross-hatched failure pattern while

OMMT/EPDM nanocomposites exhibit a typical line-flow pattern in their own fracture mechanisms.

To obtain nanocomposites with good mechanical properties, the mixing temperature, the rotor speed and the mixing time needs to be optimized for different clay concentration. The addition of OMMT improved the mechanical properties and degradation behavior of the EPDM matrix. Also, the blending conditions have some effects on these properties. As an example, increment in rotor speed for neat EPDM and EPDM/10 wt. % OMMT increased the tensile strength by 13 and 18%, respectively; however it was improved by 19% for EPDM/5 wt. % OMMT. In addition, the tensile strength of the EPDM increased by 142.1%, and 315.8%, respectively with the addition of 5 and 10 wt. % of clays into the polymer matrix for blending time of 10 min. As the effect of aging process was examined, it was observed that the better mechanical properties were observed by addition of clay. Extend of degradation was found to be improved by the addition of OMMT within the EPDM matrix. It was observed that although the reduction in the tensile strength of neat EPDM increased by increasing the blending temperature, the percentage of the loss in strength values remained almost the same for the nanocomposites. The elongation at break values increases due to increased temperature from 120°C to 150°C for neat EPDM. However, for EPDM/5 wt. % OMMT nanocomposites, as the temperature of blending increased from 120 °C to 150 °C, elongations at break values were dropped by 18 % and 23.36 %, respectively. The tensile strength, elongation at break and tensile modulus values increases due to increased rotor speed from 60 rpm to 90 rpm for neat EPDM and EPDM/10% OMMT nanocomposite while tensile modulus values remain almost constant for the same case.

The hardness values of neat EPDM and EPDM/OMMT nanocomposites before and after aging were compared. After aging, the values were decreased by about 5, 2 and 2% for neat EPDM and EPDM/OMMT nanocomposites with 5 and 10 wt. % OMMT, respectively.

When the influence of the blending temperature and blending speed were investigated, there was not any significant affect of the blending temperature and speed on the tear strength of neat EPDM and OMMT/EPDM nanocomposites. As the tear strength of 5 wt. % OMMT/EPDM nanocomposite increased slightly with time, 10 wt. % OMMT/EPDM nanocomposites showed the same behavior with neat EPDM.

TGA analysis revealed that EPDM/layered silicate nanocomposites have higher thermal stability than neat EPDM. Also, the percentage of the weight retained has

increased with an increase in organoclay loading. The T_g values were not affected by the process conditions significantly through DSC analysis. DMA results showed that EPDM/ OMMT nanocomposites exhibit higher storage modulus than neat EPDM because of the greater reinforcing effect of OMMT. The T_g value of EPDM was slightly increased from -42.39 to -40.75 °C and the value $\tan\delta_{\max}$ reduced by the addition of OMMT attributed to the nanolayers restrict the mobility of the EPDM molecular chains. On the other hand, no effects of process conditions were observed on the thermo-mechanical behavior of the composites.

REFERENCES

- Acharya, H., M. Pramanik, S. Srivastava, A. Bhowmick. 2004. Synthesis and Evaluation of High-Performance Ethylene-Propylene-DieneTerpolymer/Organoclay Nanoscale Composites. *Journal of Applied Polymer Science* 93: 2429-2436.
- Ahmadi, S., Y. Huang, W. Li. 2005. Fabrication and Physical Properties of EPDM/Organoclay Nanocomposites. *Composites Science and Technology* 65: 1069-1076.
- Bozkurt E., E. Kaya, M. Tanoğlu. 2007. Mechanical and Thermal Behavior of Non-crimp Glass Fiber Reinforced Layered Clay/Epoxy Nanocomposites. *Composites Science and Technology* 67: 3394-3403.
- Bruce, Duncam, and Dermot O'Hare, eds. 1996. *Inorganic Materials*. New York: John Wiley and Sons.
- Dai, J. and J. Huang. 1999. Surface Modification of Clays and Clay-Rubber Composite. *Applied Clay Science* 15: 51-65.
- Dick, John. 2001. *Rubber Technology: Compounding and Testing for Performance*. Munich: Hanser Publishers.
- Gatos, K., R. Thomann, J. Karger-Kocsis. 2004. Characteristics of Ethylene Propylene Diene Monomer Rubber/Organoclay Nanocomposites Resulting From Different Processing Conditions and Formulations. *Polymer International* 53: 1191-1197.
- Gatos, K. and J. Karger-Kocsis. 2005. Effects of Primary and Quaternary Amine Intercalants on the Organoclay Dispersion in a Sulfur-Cured EPDM Rubber. *Polymer* 46: 3069-3076.
- Giannelis, E. 1998. Polymer-Layered Silicate Nanocomposites: Synthesis, Properties and Applications. *Applied Organometallic Chemistry* 12: 675-680.
- Hasegawa, N. 1998. Preparation and Mechanical Properties of Polypropylene- Clay Hybrids Using a Maleic Anhydride-Modified Polypropylene Oligomer. *Journal of Applied Polymer Science* 67: 87-92.
- Hasegawa, N., H. Okamoto, M. Kawasumi, A. J. Usuki. 1999. Preparation and mechanical properties of polystyrene-clay hybrids. *Journal of Applied Polymer Science* 74: 3359-3364.
- Hasegawa, N., H. Okamoto, M. Kato, A. J. Usuki. 2000. Preparation and Mechanical Properties of Polypropylene-Clay Hybrids Based on Modified Polypropylene and Organophilic Clay. *Journal of Applied Polymer Science* 78: 1918-1922.

- Karger-Kocsis J. and C. Wu. 2004. Thermoset Rubber/Layered Silicate Nanocomposites. Status and Future Trends. *Polymer Engineering and Science* 44: 1083-1093.
- Ke Y., C. Long, Z. Qi. 1999. Crystallization, Properties, and Crystal and Nanoscale Morphology of PET-Clay Nanocomposites. *Journal of Applied Polymer Science* 71: 1139-1146.
- Ke Y.C. and P. Stroeve. 2005. *Polymer-Layered Silicate and Silica Nanocomposites*. Amsterdam:Elsevier. <http://www.science-direct.com/science/book/9780444515704> (accessed by November 6, 2007).
- Kelly P., A. Akelah, S. Qutubuddin, A. J. Moet. 1994. Reduction of Residual Stress in Montmorillonite/Epoxy Compounds. *Journal of Materials Science* 29: 2274–2280.
- Krishnamoorti R. and K. Yurekli. 2001. Rheology of Polymer Layered Silicate Nanocomposites. *Current Opinion in Colloid & Interface Science* 6: 464-470.
- Kurian M., A. Dasgupta, F. Beyer, M. Galvin. 2004. Investigation of the Effects of Silicate Modification on Polymer-Layered Silicate Nanocomposite Morphology. *Journal of Polymer Science: Part B: Polymer Physics* 42: 4075-4083.
- Kurian T., P. De, D. Tripathy, S. De, D. Peiffer. 1996. Effect of Clay on Properties of Ionic Thermoplastic Elastomer Based on EPDM. *Journal of Applied Polymer Science* 62: 1729-1734.
- LeBaron P., Z. Wang, Z. Wang, T. Pinnavaia. 1999. Polymer-layered Silicate Nanocomposites: an overview. *Applied Clay Science* 15: 11-29.
- Lepoittevin B., N. Pantoustier, M. Devalckenaere, M. Alexandre, C. Claberg, R. Jerome, C. Henrist, A. Rulmont, P. Dubois. 2003. Polymer/Layered Silicate Nanocomposites by Combined Intercalative Polymerization and Melt Intercalation: a Masterbatch Process. *Polymer* 44: 2033-2040.
- Lew C., W. Murphy, G. McNally. 2004. Preparation and Properties of Polyolefin-Clay Nanocomposites. *Polymer Engineering and Science* 44: 1027-1035.
- Liu B., Q. Ding, Q. He, J. Cai, B. Hu, J. Shen. 2006. Novel Preparation and Properties of EPDM/Montmorillonite Nanocomposites. *Journal of Applied Polymer Science* 99: 2578-2585.
- Ma Y., Y. Wu, Y. Wang, L. Zhang. 2006. Structure and Properties of Organoclay/EPDM Nanocomposites: Influence of Ethylene Contents. *Journal of Applied Polymer Science* 99: 914-919.
- Mohammad A. and G. Simon, eds. 2006. *Polymer Nanocomposites*. Cambridge: Woodhead Publishing.
- Morton, Maurice. 1987. *Rubber Technology*. New York: Van Nostrand Reinhold.

- Mousa, A. 2006. Cure Characteristics and Thermal Properties of Sulfur-Cured EPDM-Based Composites by Compounding with Layered Nano-Organoclay. *Polymer-Plastics Technology and Engineering* 45: 911-915.
- Silva C., B. Haidar, A. Vidal, J. Mische-Brendle, R. Dred, L. Vidal. 2005. Preparation of EPDM/synthetic Montmorillonite Nanocomposites by Direct Compounding. *Journal of Materials Science* 40: 1813-1815.
- Sircar, A. 1991. Analysis of Elastomer Vulcanizate Composition by TG-DTG Techniques. Presented at a meeting of the Rubber Division, Toronto: American Chemical Society.
- Standard Test Method for Rubber Property-Durometer Hardness, Deutsches Institut für Normung (DIN) 53 505.
- Standard Test Method for Rubber Property-Heat Ageing, Deutsches Institut für Normung (DIN) 53 508.
- Standard Test Method for Rubber Property-Tear Strength, Deutsches Institut für Normung (DIN) 53 507.
- Standard Test Method for Rubber Property-Tensile Strength, Deutsches Institut für Normung (DIN) 53 504.
- Usuki A., M. Kato, A. Okada, T. Kurauchi. 1997. Synthesis of polypropylene-clay hybrid. *Journal of Applied Polymer Science* 63: 137-138.
- Usuki A., A. Tukigase, M. Kato. 2002. Preparation and Properties of EPDM-Clay Hybrids. *Polymer* 43: 2185-2189.
- Trepte, Andreas. 2007. Montmorillonite structure. <http://en.wikipedia.org/wiki/Montmorillonite> (accessed March 12, 2008).
- Turi, A. 1997. *Thermal Characterization of Polymeric Materials*. London: Academic Press.
- Vaia R. A., H. Ishii, E. P. Giannelis. 1993. Synthesis and Properties of Two-Dimensional Nanostructures by Direct Intercalation of Polymer Melts in Layered Silicates. *Chemistry of Materials* 5: 1694-1696.
- Wu Y., Y. Ma, Y. Wang, L. Zhang. 2004. Effects of Characteristics of Rubber, Mixing and Vulcanization on the Structure and Properties of Rubber/Clay Nanocomposites by Melt Blending. *Macromolecular Materials and Engineering* 289: 890-894.
- Yano K., A. Usuki, A. Okada, T. Kurauchi, O. Kamigaito. 1993. Synthesis and Properties of Polyimide-Clay Hybrid. *Journal of Polymer Science Part A: Polymer Chemistry* 31: 2493-2498.
- Zanetti M., S. Lomakin, G. Camino. 2000. Polymer Layered Silicate Nanocomposites. *Macromolecular Material and Engineering* 279: 1-9.

- Zheng H., Y. Zhang, Z. Peng, Y. Zhang. 2004. Influence of the Clay Modification and Compatibilizer on the Structure and Mechanical Properties of Ethylene-Propylene-Diene Rubber/Montmorillonite Composites. *Journal of Applied Polymer Science* 92: 638-646.
- Zheng H., Y. Zhang, Z. Peng, Y. Zhang. 2004. Influence of Clay Modification on the Surface and Mechanical Properties of EPDM/Montmorillonite Nanocomposites. *Polymer Testing* 23: 217-223.
- Zilg C., R. Thomann, R. Mulhaupt, J. Finter. 1999. Polyurethane Nanocomposites Containing Laminated Anisotropic Nanoparticles Derived from Organophilic Layered Silicates. *Journal of Advanced Materials* 11: 49-52.